

## A test of statistical hadronization with exclusive rates

---

**Lorenzo Ferroni\***

*Università di Firenze & INFN*

*E-mail: ferroni@fi.infn.it*

**Francesco Becattini**

*Università di Firenze & INFN*

*E-mail: becattini@fi.infn.it*

We studied the statistical hadronization model in its full microcanonical formulation enforcing the maximal set of conservation laws: energy-momentum, angular momentum, parity, C-parity, isospin and abelian charges. The microcanonical weight (proportional to the probability) of an asymptotic channel, has been calculated in a field theory framework in order to account for relativistic effects due to the finite cluster's volume. A purposely devised Monte-Carlo method which allows to calculate efficiently the channel weight has been set up. A preliminary comparison of the model with measured exclusive rates in low energy ( $\sqrt{s} = 2.1$  GeV and 2.4 GeV)  $e^+e^-$  collisions and with branching ratios of some heavy resonance is shown.

*Critical Point and Onset of Deconfinement*

*July 3-6 2006*

*Florence, Italy*

---

\*Speaker.

## 1. Introduction

There is by now a compelling evidence that statistical hadronization model (SHM) reproduces particle abundances and transverse momentum spectra in high energy collisions ( $\sqrt{s} \gtrsim 10$  GeV) of elementary particles and heavy ions [1, 2].

However, the success of SHM, especially on elementary particles collisions, triggered much debate and it is still controversial [4, 5, 6, 7]. In fact, it is widely believed that an equilibration at the level of formed hadrons through a collisional process cannot occur because the system expands too quickly and kinetic calculations, also in heavy ion collisions, seem to confirm this [7]. Therefore, the apparent statistical equilibrium, must be an inherent property of the hadronization process itself. To account for these features of hadron production it has been proposed that the statistical equilibrium is not genuine (as was pointed out by Hagedorn many years ago [8]), but is mimicked by a special property of the quantum dynamics governing the hadronization: the so-called *phase space dominance* [6].

As will be discussed in the following, both genuine statistical equilibrium (which is the SHM fundamental ansatz) and phase space dominance are highly non-trivial hypotheses and before discussing possible mechanisms responsible for the apparent equilibrium features, it would be at least desirable to discriminate between the two aforementioned scenarios. For this purpose, it is necessary to design a more stringent test of genuine statistical equilibrium because inclusive hadron production at high energy collisions seems not to be sensitive enough to the quantitative difference between statistical hadronization and phase space dominance model.

As was proposed in [9], a hopefully more sensitive probe is provided by the rates of exclusive channels, which, being far less inclusive quantities than average hadron multiplicities, could be different enough in the two scenarios to allow drawing some conclusion.

Exclusive rates measurements are available at energies significantly below 10 GeV. A nice feature of such low energy data is that, to a very good approximation, all collision energy is spent into particle production (one single cluster at rest in the centre-of-mass frame) unlike at high energy, so that the initial kinematical state is completely known. In calculating the model prediction in this scenario, none of the relevant conservation laws, including energy-momentum, angular-momentum, parity and isospin, can be neglected, as pointed out in ref. [10].

In this work, we provided a suitable definition of the probability of asymptotic states in the SHM enforcing the maximal set of conservation laws (the full set of observables relevant to the orthochronous Poincaré group, the Isospin, the C-parity and abelian charges) and we calculated the probability of channels.

Confined states within the system have been described in a field theory framework. This is necessary in order to avoid identifying confined states as multiparticle states in a non-relativistic quantum mechanical approach (as was done in [11]), that is suitable as long as the system size is larger than the Compton wavelength of particles involved (i.e. when relativistic effects can be neglected), whereas it entails difficulties at smaller volumes.

Taking advantage of the formalism developed and of purposely devised numerical methods we made a preliminary test on  $e^+e^-$  collisions. It should be stressed, from the very beginning, that all the results we will show are preliminary and they can be consistently improved. It is also worth mentioning that we have confined ourselves to  $e^+e^-$  annihilation although the best system

to examine would be  $p\bar{p}$  annihilation at rest where much data on exclusive decays channels in 2, 3 and 4 bodies have been collected. However, the annihilation proceeds from a mostly unknown mixture of protonium atomic states and it is quite difficult to determine initial isospin and angular momenta.

We also compared the branching ratios of heavy resonances with statistical model predictions. The identification of (heavy) resonances with extended clusters is a tempting conceptual step. Hagedorn first put forward this idea in the '60s [8] laying the foundations of the Statistical Bootstrap Model. Also the MIT Bag model conceives resonances and hadrons as extended massive objects from the very beginning, giving rise to many physical consequences. It is therefore natural to make the same identification in the framework of the statistical hadronization model and check, on the basis of existing measurements, whether at least heavier resonances decay statistically into multi-hadronic channels. If this turned out to be the case, we would achieve a major confirmation of the old Hagedorn idea that resonances are in turn made of resonances and hadrons.

## 2. Statistical hadronization and phase space dominance

In the SHM, each multihadronic state within a cluster compatible with its quantum numbers is equally likely. The collection of such states defines the microcanonical ensemble of the cluster, which is then the best suited framework to evaluate observable quantities as statistical averages. Nevertheless, because of difficulties arising in microcanonical calculations and the indefiniteness of cluster's quantum numbers, a comparison with the data has been mostly made as yet by introducing simplifying assumptions, in the canonical or grand-canonical ensemble, where the numerical analysis is much easier and can be partially worked out analytically.

While in the microcanonical ensemble, one deals with mass and volume of clusters, in the canonical or grand-canonical ensemble one introduces temperature through a saddle-point expansion [11, 12]. In this framework, the model has given strikingly good predictions of average multiplicities in heavy ion collisions [2] and in elementary collisions as well [1] with only 3 free parameters, which is a minimum among hadronization models. Moreover, the hadronization temperature has been found to be constant for many kinds of reactions in a wide range of centre-of-mass energies, around 160 MeV [13], intriguingly close to the estimated critical temperature of QCD for the phase transition between hadron gas and *Quark-Gluon Plasma* (QGP).

As pointed out in the introduction, its apparent success in reproducing observables related to the hadronization process triggered some debate about the interpretation of the model [4, 5, 6, 7] since it is widely believed that an equilibration cannot occur after hadronization through inelastic hadron collisions [7]. Therefore, there have been some attempts to explain why we observe this statistical features in hadron production. A very interesting new idea has been recently put forward in [5, 14] where the author argues an analogy between thermal radiation in the Unruh-Hawking effect and hadron production in high energy collisions.

Apart from explanations based on other physical models, two main options arise to account for these observations:

- **Genuine statistical equilibrium:** it is an inherent property of hadronization itself, i.e. hadrons are born at equilibrium within a finite volume. This implies a spacial extension of the hadron-emitting source as in SHM.

- Phase space dominance: the apparent thermal-like features are an effect of a special property of the quantum dynamics governing hadronization, which tends to evenly populate all final states [6].

The basis of the latter argument is the similarity between the (classical) phase space volume of a set of particles, or *channel*,  $\{N_j\} \equiv N_1, \dots, N_k$  (where  $N_j$  stands for the multiplicity of the species  $j$ ) and the general expression of the decay rate of a massive particle (cluster) in relativistic quantum mechanics.

If we let  $P$  be the initial four-momentum,  $V$  the volume and let  $p_n \equiv (\varepsilon_n, \mathbf{p}_n)$  be the four momentum of the particle  $n$ ; the phase space volume  $\Omega_{\{N_j\}}$  of the channel  $\{N_j\}$  turns out to be [11] (in Boltzmann statistics):

$$\Omega_{\{N_j\}} = \frac{V^N}{(2\pi)^{3N}} \left\{ \prod_{j=1}^k \frac{1}{N_j!} \left[ \int d^3\mathbf{p} \right]^{N_j} \right\} \delta^4 \left( P - \sum_{n=1}^N p_n \right) \quad (2.1)$$

where  $N = \sum_j N_j$ . This quantity is proportional to the probability of observing the channel  $\{N_j\}$  as a consequence of the decay of a cluster of volume  $V$  and momentum  $P$ .

On the other hand, the expression of the decay rate into the channel  $\{N_j\}$  of a massive particle in relativistic quantum mechanics reads:

$$\Gamma_{\{N_j\}} = \frac{1}{(2\pi)^{3N}} \left\{ \prod_{j=1}^k \frac{1}{N_j!} \left[ \int \frac{d^3\mathbf{p}}{2\varepsilon_j} \right]^{N_j} \right\} \delta^4 \left( P - \sum_{n=1}^N p_n \right) |M_{fi}|^2 \quad (2.2)$$

where  $M_{fi}$  is the Lorentz-invariant dynamical matrix element governing the decay. Assuming, for sake of simplicity, spinless particles,  $|M_{fi}|^2$  may in principle depend on all relativistic invariants formed out of the four-momenta of the  $N$  particles, as well as on all possible isoscalars formed out of the isovector operators. Nevertheless, if we assume  $M_{fi}$  to be weakly dependent on kinematical variables, expression (2.2) becomes quite similar to (2.1) were not for the invariant measure (the so-called *invariant momentum space*  $d^3\mathbf{p}/2\varepsilon$  instead of the proper phase space  $Vd^3\mathbf{p}$ ) and for the absence of any parameter connected to spacial extension.

This phenomenon is called *phase space dominance* because the decay rate is governed by the available phase space volume rather than dynamical matrix element. For instance, if we assume that  $|M_{fi}|^2 = \alpha^N$ , i.e. the whole dynamics reduces to the same multiplicative constant  $\alpha$  for each particle in the channel, it can be then shown that the expression of the mean number of particles of the species  $j$  is well approximated by, at large  $N$ :

$$\langle n \rangle_j \simeq \frac{\alpha}{(2\pi)^3} \int \frac{d^3\mathbf{p}}{2\varepsilon_j} e^{-\beta\varepsilon_j} \quad (2.3)$$

which is very similar to a thermal distribution which one obtains from (2.1) at large multiplicities:

$$\langle n \rangle_j \simeq \frac{V}{(2\pi)^3} \int d^3\mathbf{p} e^{-\beta\varepsilon_j} \quad (2.4)$$

where  $\beta = 1/T$  is the inverse temperature. Conversely the constant  $\beta$  in Eq. (2.3) is not a temperature, rather a parameter which is related to the hadronization scale. Yet, the ratios of average

multiplicities of particles of different species mimic a thermodynamic behavior. The authors of ref. [6] work out a more specific example based on QED and they conclude, quite reasonably, that a fairly good fit to particle multiplicities may be obtained if integral expressions like (2.3) are used instead of an actual Boltzmann integral.

It should be emphasized that phase space dominance is a highly non-trivial assumption. In fact, the recovery of a thermal-like expression like (2.3) owes to a very special form of the matrix element  $|M_{fi}|^2$ , where both the dependence on kinematical and isospin invariants was disregarded. If a different form, still perfectly legitimate and possible, is assumed, the thermal-like behavior is spoiled. Therefore, an observed phase space dominance in multihadron production is not a trivial fact and tells us something important about the characteristics of non perturbative QCD dynamics, besides providing us with an empirically good model.

### 3. A crucial test: exclusive rates

In the light of the arguments discussed in last section we conclude that a deeper test of the model is needed in order to identify a genuine statistical-thermal behaviour and distinguish between it and possible pseudo-statistical models like phase space dominance. We need to investigate observables more sensitive to distinctive features of the SHM. It would be then desirable to bring out effects related to finite volume, which is a peculiarity of the statistical model. Indeed, the study of average inclusive multiplicities or inclusive  $p_T$  spectra does not allow to draw clearcut conclusions because these observables are not sensitive enough to different integration measures (i.e.  $Vd^3p$  versus  $d^3p/2\varepsilon$  respectively in (2.4) and (2.3)) and much information is integrated away.

As has been proposed in [9], a much more effective test would be studying the production rates of exclusive channels of a collision, i.e.  $\Gamma_{\{N_j\}}/\Gamma_{\{N'_j\}}$ , that is the relative probability of observing a well defined set of particles (channel) in the final state of a collision. Thereby, we would compare directly with the experimental data expressions like (2.1) and (2.2) which are more sensitive to the integration measure in the momentum integrals and the shape of dynamical matrix element.

Unfortunately, exclusive channels can be measured only at low energy ( $\sqrt{s} \sim \text{few GeV}$ ) since the number and the complexity of final states become quickly prohibitive, from the experimental point of view, as centre-of-mass energy increases. This energy range is well below the perturbative scale to let us argue that any perturbative effect (like e.g. *jets* formation and kinematical anisotropies), eventually leading to a multi-cluster scenario, should not show up.

It can be therefore assumed, that in the final state of a low energy (some GeV) collision, one single cluster is formed at rest in the centre-of-mass frame (see fig. (1)); where cluster's mass and internal quantum numbers are fixed by  $\sqrt{s}$  and initial state conditions. At such low energies, none of the relevant conservation laws, including angular momentum, parity and isospin, can be neglected, as pointed out in ref. [10] where  $p\bar{p}$  annihilation at rest was studied in this approach. This makes calculations rather cumbersome and hard from the numerical point of view. None of the many previous studies in literature (among the others [15]) has tackled the problem without introducing approximations which unavoidably implied large errors in the calculations. The microcanonical partition function of a relativistic gas with angular momentum conservation has been calculated in [16] by using a projection method. Although this work represents the best attack to the problem to date, the final expression has been obtained in a large-volume approximation and

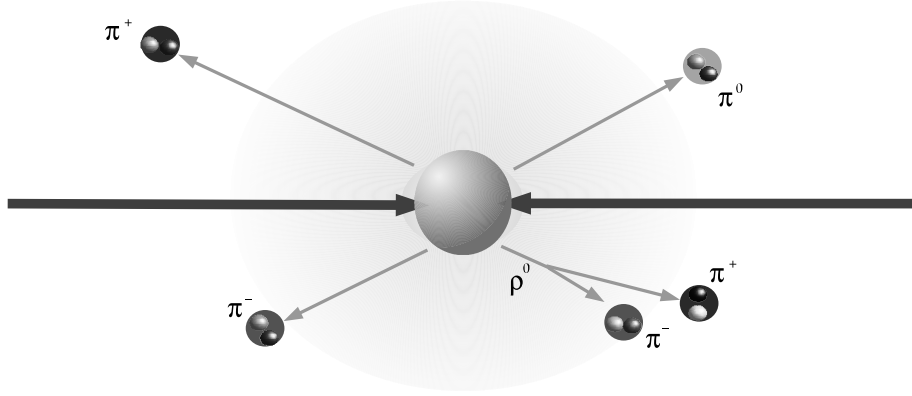


**Figure 1:** Pictorial representation of a low energy ( $\lesssim 5$  GeV) collision in the statistical model. One single cluster is formed at rest with a mass  $M = \sqrt{s}$  and with quantum numbers given by the initial state conditions.

only for spinless particles. Fully microcanonical calculations including both four-momentum and angular momentum conservation have not ever been done, and only recently the increased computing power and purposely designed techniques allowed the calculation of averages in the hadronic microcanonical ensemble, though only with energy and momentum conservation [17, 18, 12].

The first, fundamental, problem to face is how to write the probability of a channel  $\{N_j\}$  when all conservation laws are enforced. We must thus provide a formulation of the SHM in the full microcanonical ensemble of the relativistic hadron gas, where all conserved quantities in strong interaction are constrained.

#### 4. Probability of states in the statistical hadronization model

The definition of a probability of a channel, or a general final state, in the SHM is not straightforward as it might seem, in spite of the simplicity of the key assumptions of the model. In fact, the basic postulate tells us that *localized states* compatible with cluster's quantum numbers are equiprobable, but these states do not coincide with observable free-particle asymptotic states. Such difference is, for practical purposes, not an issue when the volume is sufficiently large and can thus be disregarded in most applications where the canonical or grand-canonical ensemble are used. Yet, it is relevant in principle and may result in quantitative differences when the volume is comparable with the pion Compton wavelength, i.e. less than  $\mathcal{O}(10)$  fm<sup>3</sup>, as in the case of low energy collision of our interest. In such a situation one should, in principle, take into account that confined states within the cluster cannot be identified with multiparticle asymptotic states.

The SHM assumes that the cluster can be described as a normal statistical mixture of multi-hadronic states compatible with its initial quantum numbers. Accordingly, if we confine ourselves to energy-momentum conservation, we can write down a microcanonical partition function  $\Omega$ , which is defined as the collection of all states within the cluster volume  $V$  with total four-momentum equal to the cluster's four momentum  $P$ :

$$\Omega = \sum_{h_V} \langle h_V | \delta^4(P - \hat{P}) | h_V \rangle, \quad (4.1)$$

where  $\widehat{P}$  is the four momentum operator<sup>1</sup> and the set  $\{|h_V\rangle\}$  is a generic basis of the localized system. Eq. (4.1) can be generalized by replacing  $\delta^4(P - \widehat{P})$  with a generic projector  $P_i$  over all conserved quantities:

$$\Omega = \sum_{h_V} \langle h_V | P_i | h_V \rangle. \quad (4.2)$$

The states  $|h_V\rangle$  in (4.2) are not the observable asymptotic free states  $|f\rangle$  of the Fock space. Instead, a suitable probability definition should involve these states. To do this, one can recast the microcanonical partition function (4.2) by using the completeness of states  $|f\rangle$ :

$$\Omega = \sum_{h_V} \langle h_V | \sum_f |f\rangle \langle f| P_i | h_V \rangle = \sum_f \langle f | P_i \sum_{h_V} |h_V\rangle \langle h_V | f \rangle \equiv \sum_f \langle f | P_i P_V | f \rangle \quad (4.3)$$

where  $P_V = \sum_{h_V} |h_V\rangle \langle h_V|$  is the projector onto localized states. We note that the last expression of  $\Omega$  in Eq. (4.3) is a proper trace, whereas it was not in Eq. (4.2) as the states  $|h_V\rangle$  do not form a complete set of the full Hilbert space.

The quantity:

$$\rho_f \equiv \langle f | P_i P_V | f \rangle \quad (4.4)$$

is the *microcanonical state weight* of the asymptotic state  $|f\rangle$ . It can be proved that, in the rest frame of the cluster (i.e.  $P = (M, \mathbf{0})$ ), if we assume a spherically symmetric shape (actually we will assume clusters to be sharp spheres),  $\rho_f$  (up to a normalizing constant  $1/\Omega$ ) fulfills all needed requirements of a good definition of probability for the ideal hadron gas [19].

In order to calculate  $\rho_f$ , it is convenient to insert a resolution of the identity by using again the completeness of a set of Fock states  $|f'\rangle$ 's:

$$\rho_f \equiv \sum_{f'} \langle f | P_i | f' \rangle \langle f' | P_V | f \rangle \quad (4.5)$$

and work out the matrix elements  $\langle f | P_i | f' \rangle$  and  $\langle f' | P_V | f \rangle$  separately.

The projector  $P_i$  is the projector onto an irreducible state of the orthochronous Poincaré group  $\text{IO}(1,3)^\uparrow$ <sup>2</sup> and of the internal symmetry group, that is, in our case, the isospin group  $\text{SU}(2)$  and  $\text{U}(1)$ 's related to baryon number and strangeness; in other words, we assume  $\text{SU}(3)$  flavour symmetry to be completely broken, i.e.  $\text{SU}(3) \rightarrow \text{SU}(2) \otimes \text{U}(1)$ .  $P_i$  can be then written as:

$$P_i = P_{PJ\lambda\Pi} P_{I_3} P_C P_Q \quad (4.6)$$

where  $I$  and  $I_3$  are the isospin and its third component and

$$P_{I_3} = |I, I_3\rangle \langle I, I_3|; \quad (4.7)$$

$C$  is the C-parity<sup>3</sup> and

$$P_C |f\rangle = \frac{1+C\widehat{C}}{2} |f\rangle, \quad (4.8)$$

<sup>1</sup>Note that in what follows operators will be distinguished from ordinary numbers by a “ $\widehat{\phantom{x}}$ ”.

<sup>2</sup>Strictly speaking, projection operators cannot be defined for non-compact groups, nevertheless, we will maintain this naming relaxing mathematical rigor.

<sup>3</sup>Of course, the projection  $P_C$  makes sense only if  $I_3 = 0$  and  $\mathbf{Q} = \mathbf{0}$ ; in this case,  $P_C$  commutes with all other projectors

where  $C$  is the charge conjugation operator and  $\widehat{C}$  its unitary representation. In Eq. (4.6),  $\mathbf{Q} = (Q_1, \dots, Q_M)$  is a set of  $M$  abelian charges (in fact they are 2, baryon number and strangeness) and  $P_{PJ\lambda\Pi}$  is the projector over the maximal set of space-time observables (four-momentum  $P$ ; spin  $J$  and its third component  $\lambda$ ; parity  $\Pi$ ), i.e. an irreducible state of the orthochronous Poincaré group  $\text{IO}(1,3)^\dagger$ :

$$P_{PJ\lambda\Pi} = \frac{1}{2} \sum_{z=1,\Pi} \dim v \int d\mu(g_z) D_{ii}^{v\dagger}(g_z) \hat{g}_z \quad (4.9)$$

where  $\mu$  is the invariant group measure,  $z$  is the identity or space inversion  $\Pi$ ,  $g_z \in \text{IO}(1,3)^\dagger_\pm$ ,  $D^v(g_z)$  is the matrix of the unitary irreducible representation  $v$  pertaining to the state  $i$ , and  $\hat{g}_z$  is the unitary representation of  $g_z$  in the Hilbert space. Working in the rest frame of the system, with  $P = (M, \mathbf{0})$ , the matrix element  $D_{ii}^{v\dagger}(g_z)$  vanishes unless Lorentz transformations are pure rotations and this implies the reduction of the integration in (4.9) from  $\text{IO}(1,3)^\dagger$  to the subgroup  $\text{T}(4) \otimes \text{SU}(2) \otimes \text{Z}_2$  [11] (replacing  $\text{SO}(3)$  with universal covering group  $\text{SU}(2)$ ). Therefore, it can be proved that  $P_{PJ\lambda\Pi}$  reduces to [11]:

$$P_{PJ\lambda\Pi} = (2J+1) \delta^4(P - \widehat{P}) \int dR D_{\lambda\lambda}^J(R^{-1}) \widehat{R} \frac{1 + \Pi \widehat{\Pi}}{2}, \quad (4.10)$$

$dR$  being the invariant  $\text{SU}(2)$  measure normalized to 1,  $\Pi$  being the parity of the system and  $\widehat{\Pi}$  is the spacial inversion operator unitary representation. The appeal of the above expression resides in the factorization of projections onto the energy-momentum  $P$ , spin-helicity  $J, \lambda$  and parity  $\Pi$  which allows us to calculate the contribution of angular momentum and energy-momentum conservation separately.

The other projector appearing in Eq. (4.5) is the projector on a finite volume  $P_V$ . According to its definition,  $P_V$ , is the projector identity as far as internal symmetries are concerned and it commutes with the projectors  $P_C P_{I,3} P_Q$ . The situation is rather different for space-time symmetries. In fact rotation and space inversion operators commute with  $P_V$  provided the system is spherical in shape, while space-time translation symmetry is not fulfilled because of the finite volume.

According to the discussion at the beginning of this section, we defined  $P_V$  in a quantum field theory framework identifying localized states as states  $|\psi\rangle$  of the quantum field operator  $\Psi$  associated to particles vanishing out of the system region. This has been done in order to avoid describing confined states as multiparticle states, which entails difficulties when the volume is small. In fact, particle number operators in the whole space are essentially different from those in a finite region. As an example, an  $N$ -pion state in a finite region has non vanishing components on *all* free states of the pion field, i.e. on the states with  $0, 1, 2, \dots$  pions. This problem is mostly known to physicists as expounded by Landau [20]: when trying to localize an electron, electron-position pairs unavoidably appear.

Confined states have been then described in a proper quantum relativistic field theory framework in order to account for these relativistic effects related to the finite size of the system. For instance, in case of only one scalar particle:

$$P_V = \int_V \mathcal{D}\psi |\psi\rangle \langle \psi| \quad (4.11)$$

where  $|\Psi\rangle \equiv \otimes_{\mathbf{x}} |\psi(\mathbf{x})\rangle$  and  $\mathcal{D}\Psi$  is the functional measure; the index  $V$  means that the functional integration must be performed over all functions having as support the system region  $V$ . A generalization of Eq. (4.11) to particles endowed with spin can be obtained by using a definition for general charged fields (in Schrödinger representation) corresponding to particles (either bosons or fermions) with spin  $S$  given in [21]:

$$\begin{aligned}\Psi_{\tau}(\mathbf{x}) &= \frac{1}{(2\pi)^{\frac{3}{2}}} \int \frac{d^3\mathbf{p}}{\sqrt{2\varepsilon}} D_{\tau\sigma}^S([p]) a(p, \sigma) e^{i\mathbf{p}\cdot\mathbf{x}} + D_{\tau\sigma}^S([p]C^{-1}) b^{\dagger}(p, \sigma) e^{-i\mathbf{p}\cdot\mathbf{x}} \\ \tilde{\Psi}_{\tau}(\mathbf{x}) &= \frac{1}{(2\pi)^{\frac{3}{2}}} \int \frac{d^3\mathbf{p}}{\sqrt{2\varepsilon}} D_{\tau\sigma}^S([p]^{\dagger-1}) a(p, \sigma) e^{i\mathbf{p}\cdot\mathbf{x}} + D_{\tau\sigma}^S([p]^{\dagger-1}C) b^{\dagger}(p, \sigma) e^{-i\mathbf{p}\cdot\mathbf{x}}\end{aligned}\quad (4.12)$$

where  $\varepsilon = \sqrt{p^2 + m^2}$  is the 0-th component of the four momentum  $p$ ;  $a$ ,  $a^{\dagger}$  and  $b$ ,  $b^{\dagger}$  are respectively annihilation and creation operators for particles and antiparticles and  $[p]$  denotes the  $\text{SL}(2, \mathbb{C})$  matrix which transforms  $p^0 = (m, \mathbf{0})$  to  $p = (\varepsilon, \mathbf{p})$ . The transformation  $C$  in the last equation, if understood as the corresponding matrix  $C \equiv i\sigma_2$ , fulfills the following properties:

$$C = C^T = C^*, \quad C^2 = -1 \quad \text{and} \quad CAC^{-1}A^T = I(\det A) \quad (4.13)$$

for  $A \in \text{SL}(2, \mathbb{C})$  and gives the spin-statistics connection :

$$D_{\tau\sigma}^S(C^2) = (-1)^{2S} \delta_{\tau, \sigma} . \quad (4.14)$$

Fields  $\Psi$  and  $\tilde{\Psi}$  are also correct degrees of freedom for neutral particles, provided  $b^{\dagger}$ 's operators are replaced with  $a^{\dagger}$  in 4.12 [21]. We will thus write the projector on a finite volume  $P_V$  as:

$$P_V = \int_V \mathcal{D}\Psi \mathcal{D}\tilde{\Psi} |\Psi, \tilde{\Psi}\rangle \langle \Psi, \tilde{\Psi}| . \quad (4.15)$$

Let us now first evaluate the matrix elements of  $P_V$  and  $P_i$  on single particle states  $|f\rangle \equiv |p, \sigma\rangle$  and  $|f'\rangle \equiv |p', \sigma'\rangle$ . For sake of simplicity, we omit to enforce parity, C-parity and isospin conservation, i.e. we let:

$$P_i \equiv P_{PJ\lambda} = \delta^4(P - \hat{P})(2J + 1) \int dR D_{\lambda\lambda}^J(R^{-1}) \hat{R} . \quad (4.16)$$

By using the same notation of [21], the matrix element of  $P_{PJ\lambda}$  on single particle states will be written as [19]:

$$\langle p, \sigma | P_{PJ\lambda} | p', \sigma' \rangle = \delta^4(P - p')(2J + 1) \int dR D_{\lambda\lambda}^J(R^{-1}) \delta^3(\mathbf{R}\mathbf{p}' - \mathbf{p}) D_{\sigma\sigma'}^S([Rp']^{-1}R[p']) \quad (4.17)$$

where  $S$  is the spin of the particle and  $[Rp']^{-1}R[p']$  is a Wigner rotation.

The matrix element of  $P_V$  in (4.15) can be evaluated on single particle states as well by introducing creation and annihilation operators and expressing them in terms of field operators by

using the relations:

$$\begin{aligned}
\langle 0|a(p, \sigma) &= \langle 0| \frac{1}{(2\pi)^{\frac{3}{2}}} \int d^3x e^{-i\mathbf{p}\cdot\mathbf{x}} \sqrt{2\varepsilon} D_{\sigma\tau}^S([p]^{-1}) \Psi_{\tau}(\mathbf{x}) & (4.18) \\
a^{\dagger}(p, \sigma)|0\rangle &= \frac{1}{(2\pi)^{\frac{3}{2}}} \int d^3x e^{i\mathbf{p}\cdot\mathbf{x}} \sqrt{2\varepsilon} \tilde{\Psi}_{\tau}^{\dagger}(\mathbf{x}) D_{\tau\sigma}^S([p]) |0\rangle \\
\langle 0|b(p, \sigma) &= \langle 0| \frac{1}{(2\pi)^{\frac{3}{2}}} \int d^3x e^{-i\mathbf{p}\cdot\mathbf{x}} \sqrt{2\varepsilon} \tilde{\Psi}_{\tau}^{\dagger}(\mathbf{x}) D_{\tau\sigma}^S([p]C) \\
b^{\dagger}(p, \sigma)|0\rangle &= \frac{1}{(2\pi)^{\frac{3}{2}}} \int d^3x e^{i\mathbf{p}\cdot\mathbf{x}} \sqrt{2\varepsilon} D_{\sigma\tau}^S(C[p]^{-1}) \Psi_{\tau}(\mathbf{x}) |0\rangle
\end{aligned}$$

which follow from the definition (4.12). By using (4.18) the matrix element of  $P_V$  between two one-particle free states can be worked out as:

$$\begin{aligned}
\langle p', \sigma' | P_V | p, \sigma \rangle &= \langle 0 | a(p', \sigma') P_V a^{\dagger}(p, \sigma) | 0 \rangle & (4.19) \\
&= \frac{1}{(2\pi)^3} \int d^3x d^3x' e^{-i\mathbf{p}'\cdot\mathbf{x}'} e^{i\mathbf{p}\cdot\mathbf{x}} 2\sqrt{\varepsilon\varepsilon'} D_{\sigma'\tau'}^S([p']^{-1}) D_{\tau\sigma}^S([p]) \langle 0 | \Psi_{\tau'}(\mathbf{x}') P_V \tilde{\Psi}_{\tau}^{\dagger}(\mathbf{x}) | 0 \rangle
\end{aligned}$$

and, using the definition (4.15), the vacuum expectation value on the right-hand side as:

$$\langle 0 | \Psi_{\tau'}(\mathbf{x}') P_V \tilde{\Psi}_{\tau}^{\dagger}(\mathbf{x}) | 0 \rangle = \int_V \mathcal{D}\psi \mathcal{D}\tilde{\psi} \psi_{\tau'}(\mathbf{x}') |\langle 0 | \psi, \tilde{\psi} \rangle|^2 \tilde{\psi}_{\tau}^{\dagger}(\mathbf{x}). \quad (4.20)$$

Notice that in the limit  $V \rightarrow \infty$ , since  $P_V \rightarrow 1$ , the expression in (4.20) reduces to a well known expression in field theory, the two point correlation function:

$$\langle 0 | \Psi_{\tau'}(\mathbf{x}') \tilde{\Psi}_{\tau}^{\dagger}(\mathbf{x}) | 0 \rangle = \int \mathcal{D}\psi \mathcal{D}\tilde{\psi} \psi_{\tau'}(\mathbf{x}') |\langle 0 | \psi, \tilde{\psi} \rangle|^2 \tilde{\psi}_{\tau}^{\dagger}(\mathbf{x}). \quad (4.21)$$

The factor  $|\langle 0 | \psi, \tilde{\psi} \rangle|^2$  is the squared modulus of the *vacuum functional* and reads (up to a constant factor) [22]:

$$|\langle 0 | \psi, \tilde{\psi} \rangle|^2 = \exp \left\{ -\frac{1}{2} \int d^3x_1 d^3x_2 \tilde{\psi}^{\dagger}(\mathbf{x}_1) K(\mathbf{x}_1 - \mathbf{x}_2) \psi(\mathbf{x}_2) + \psi^{\dagger}(\mathbf{x}_2) K(\mathbf{x}_1 - \mathbf{x}_2) \tilde{\psi}(\mathbf{x}_1) \right\}, \quad (4.22)$$

where  $K$  is the *kernel*. Eq. (4.21) is thus a gaussian integral whose solution is:

$$\langle 0 | \Psi_{\tau'}(\mathbf{x}') \tilde{\Psi}_{\tau}^{\dagger}(\mathbf{x}) | 0 \rangle = I_0 K^{-1}(\mathbf{x}' - \mathbf{x})_{\tau'\tau} \quad (4.23)$$

where  $K^{-1}$  is the inverse kernel and  $I_0 \equiv \langle 0 | 0 \rangle$  a constant factor [22]. When the volume is finite, the functional integral in (4.20) is still gaussian and can be solved by finding the inverse of the kernel over the finite region  $V$ . Then, the Eq. (4.19) turns out to be:

$$\begin{aligned}
\langle p', \sigma' | P_V | p, \sigma \rangle &= \frac{1}{(2\pi)^3} \int_V d^3x e^{i\mathbf{x}\cdot(\mathbf{p}-\mathbf{p}')} \sqrt{\frac{\varepsilon}{\varepsilon'}} D_{\sigma'\sigma}^S([p']^{-1}[p]) & (4.24) \\
&\equiv \sqrt{\frac{\varepsilon}{\varepsilon'}} F_V(\mathbf{p}-\mathbf{p}') D_{\sigma'\sigma}^S([p']^{-1}[p])
\end{aligned}$$

where  $F_V$  in Eq. (4.24) is a Fourier integral over the system region  $V$ :

$$F_V(\mathbf{p} - \mathbf{p}') = \frac{1}{(2\pi)^3} \int_V d^3x e^{i\mathbf{x} \cdot (\mathbf{p} - \mathbf{p}')} . \quad (4.25)$$

Eq. (4.24) is indeed the same result which has been obtained in ref. [11] in a non-relativistic quantum mechanical (NRQM) framework. The NRQM result is also found when considering states composed by many (identical) particles (or particle-antiparticle pairs) provided that divergent additional terms which appear in some cases can be safely subtracted away. The appearance of such divergences is tightly related to the field formalism (for a detailed discussion see ref. [19]). Nevertheless, retaining the definition ((4.15)), it is possible to subtract “by hand” these divergencies in a consistent way and then recover the NRQM result with no additional terms.

The state weight  $\rho_f$  can be thus calculated for a generic final state, taking into account that, when considering groups of identical particles, one can work on the multiparticle tensor space including Bose or Fermi statistics. In the simple case of  $N$  distinct particles, if we let  $\{p_n\}$  and  $\{\lambda_n\}$  be the set of four-momenta and helicities (or polarizations) of particles, the state weight  $\rho_f$  reads:

$$\rho_f = (2J+1) \int dR D_{\lambda\lambda}^J(R^{-1}) \delta^4 \left( P - \sum_{n=1}^N p_n \right) \left[ \prod_{n=1}^N D_{\lambda_n \lambda_n}^{S_n}([p_n]^{-1} R[p_n]) F_V(\mathbf{p}_n - R^{-1} \mathbf{p}_n) \right] , \quad (4.26)$$

whereas for a generic state with  $\{N_j\}$  particles, if we let  $\{N_j\} \equiv N_1, \dots, N_k$  be the set of multiplicities of the hadron species  $1, \dots, k$ , the corresponding expression turns out to be:

$$\begin{aligned} \rho_f &= (2J+1) \sum_{\{\rho_j\}} \left[ \prod_{j=1}^k \chi(\rho_j)^{b_j} \right] \int dR D_{\lambda\lambda}^J(R^{-1}) \delta^4 \left( P - \sum_{n=1}^N p_n \right) \\ &\times \prod_{j=1}^k \left[ \prod_{n_j=1}^{N_j} D_{\lambda_{n_j} \lambda_{\rho(n_j)}}^{S_j}([p_{n_j}]^{-1} R[p_{\rho(n_j)}]) F_V(\mathbf{p}_{\rho(n_j)} - R^{-1} \mathbf{p}_{n_j}) \right] \end{aligned} \quad (4.27)$$

where the index  $n$  labels the whole set of  $N \equiv \sum_{j=1}^k N_j$  particles in the channel and  $n_j$  labels particles of species  $j$ . In Eq. (4.27)  $\{\rho_j\}$  stands for the set of permutations  $\rho_1, \dots, \rho_k$ , where  $\rho_j$  is a permutation of the integers  $1, \dots, N_j$ ,  $\chi(\rho_j)$  its parity and  $b_j = 0; 1$  for bosons and fermions respectively. Eq. (4.27) is the microcanonical state weight with four-momentum and angular momentum conservation.

## 5. Probability of a single channel

Summing  $\rho_f$  over all kinematical variables (momenta and helicities) of particles one can get the microcanonical weight of a channel (or *channel weight*), thence its probability by normalizing with  $1/\Omega$ . For a set of distinguishable particles the microcanonical weight  $\Omega_N$  can be calculated from Eq. (4.26) by integrating  $\rho_f$  over all particles momenta and summing over their polarizations:

$$\begin{aligned} \Omega_N &= (2J+1) \int dR D_{\lambda\lambda}^J(R^{-1}) \left[ \prod_{n=1}^N \int d^3p_n \right] \delta^4 \left( P - \sum_{n=1}^N p_n \right) \\ &\times \left[ \prod_{n=1}^N \text{tr} [D^{S_n}(R)] F_V(\mathbf{p}_n - R^{-1} \mathbf{p}_n) \right] \end{aligned} \quad (5.1)$$

where we used the cyclicity property of the trace:

$$\text{tr} [D^{S_n}([p_n]^{-1}R[p_n])] = \text{tr} [D^{S_n}(R)] . \quad (5.2)$$

For a generic state with a set  $\{N_j\}$  of particles, by recalling that any permutation  $\rho_j$  of  $N_j$  integers can be uniquely decomposed into the product of cyclic permutations, that is  $\rho_j = c_1 \dots c_{H_j}$ , one similarly obtains, from (4.27):

$$\begin{aligned} \Omega_{\{N_j\}} &= (2J+1) \sum_{\{\rho_j\}} \left[ \prod_{j=1}^k \frac{\chi(\rho_j)^{b_j}}{N_j!} \right] \int dR D_{\lambda\lambda}^J(R^{-1}) \left[ \prod_{j=1}^k \prod_{n_j=1}^{N_j} \int d^3 p_{n_j} \right] \\ &\times \delta^4 \left( P - \sum_{n=1}^N p_n \right) \prod_{j=1}^k \left[ \prod_{n_j=1}^{N_j} \text{tr} [D^{S_j}(R^{n_j})]^{h_{n_j}(\rho_j)} F_V(\mathbf{p}_{\rho_j(n_j)} - R^{-1}\mathbf{p}_{n_j}) \right] \end{aligned} \quad (5.3)$$

where  $h_{n_j}(\rho_j)$  is the number of cyclic permutations  $c_{n_j}$  with  $n_j$  elements in  $\rho_j$  such that  $\sum_{n_j=1}^{\infty} n_j h_{n_j} = N_j$ <sup>4</sup>.

As one can realize, in both Eq. (5.1) and (5.3), the Wigner rotations matrices resulting from the matrix element of  $P_{P_{J\lambda}}$  in (4.17) and Lorentz transformation matrices resulting from the matrix element of  $P_V$  in (4.24), combine in such a way that one is left with a trace of simple SU(2) rotations in the expression of the channel weight. This is indeed a crucial point which simplifies a lot calculations.

Eq. (5.3) can be further developed by recalling that the trace of a rotation is the same for all rotations belonging to the same conjugacy class which is, in SU(2), the set of all rotations of the same angle  $\psi$  around an axis  $\hat{\mathbf{n}}$ , which labels the different members of the conjugacy class. It is therefore convenient to use the axis-angle parametrization for the integration over the SU(2) group and use the corresponding invariant integration measure, i.e.:

$$\int dR = \frac{1}{16\pi^2} \int_0^\pi d\theta \int_0^{2\pi} d\phi \int_0^{4\pi} d\psi 2 \sin \theta \sin^2 \frac{\psi}{2} = \frac{1}{16\pi^2} \int d\Omega_{\hat{\mathbf{n}}} \int_0^{4\pi} d\psi 2 \sin^2 \frac{\psi}{2} \quad (5.4)$$

where  $(\theta, \phi)$  are the polar and azimuthal angles defining the axis  $\hat{\mathbf{n}}$ . With this parametrization, the trace of a rotation  $R_{\hat{\mathbf{n}}}(\psi)$  reads:

$$\text{tr} [D^S(R_{\hat{\mathbf{n}}}(\psi))] = \frac{\sin[(S + \frac{1}{2})\psi]}{\sin \frac{\psi}{2}} \quad (5.5)$$

and the Eq. (5.3):

$$\begin{aligned} \Omega_{\{N_j\}} &= (2J+1) \sum_{\{\rho_j\}} \left[ \prod_{j=1}^k \frac{\chi(\rho_j)^{b_j}}{N_j!} \right] \frac{1}{8\pi^2} \int d\Omega_{\hat{\mathbf{n}}} \int_0^{4\pi} d\psi \sin^2 \frac{\psi}{2} D_{\lambda\lambda}^J(R_{\hat{\mathbf{n}}}^{-1}(\psi)) \left[ \prod_{j=1}^k \prod_{n_j=1}^{N_j} \int d^3 p_{n_j} \right] \\ &\times \delta^4 \left( P - \sum_{n=1}^N p_n \right) \prod_{j=1}^k \left[ \prod_{n_j=1}^{N_j} \left[ \frac{\sin[(S_j + \frac{1}{2})n_j\psi]}{\sin(\frac{n_j\psi}{2})} \right]^{h_{n_j}(\rho_j)} F_V(\mathbf{p}_{\rho_j(n_j)} - R_{\hat{\mathbf{n}}}^{-1}(\psi)\mathbf{p}_{n_j}) \right] . \end{aligned} \quad (5.6)$$

<sup>4</sup>The set of integers  $h_1, \dots, h_{N_j} \equiv \{h_{n_j}\}$ , is usually defined as a *partition* of the integer  $N_j$  in the multiplicity representation.

If we assume the cluster to be a sharp sphere in shape (actually it is sufficient to assume spherically symmetric shape), the channel weight turns out to be independent on the polarization  $\lambda$  so that, after summing over  $\lambda$ , the integrand in (5.6) is independent on the rotation axis  $\hat{\mathbf{n}}$  [19] and one can therefore integrate away the solid angle  $\Omega_{\hat{\mathbf{n}}}$  and comfortably choose  $\hat{\mathbf{z}}$  as a rotation axis:

$$\begin{aligned} \Omega_{\{N_j\}} &= (2J+1) \sum_{\{\rho_j\}} \left[ \prod_{j=1}^k \frac{\chi(\rho_j)^{b_j}}{N_j!} \right] \frac{1}{2\pi} \int_0^{4\pi} d\psi \sin \frac{\psi}{2} \sin \left[ \left( J + \frac{1}{2} \right) \psi \right] \left[ \prod_{j=1}^k \prod_{n_j=1}^{N_j} \int d^3 \mathbf{p}_{n_j} \right] \\ &\times \delta^4 \left( P - \sum_{n=1}^N p_n \right) \prod_{j=1}^k \left[ \prod_{n_j=1}^{N_j} \left[ \frac{\sin[(S_j + \frac{1}{2})n_j \psi]}{\sin(\frac{n_j \psi}{2})} \right]^{h_{n_j}(\rho_j)} F_V^\circ(\mathbf{p}_{\rho_j(n_j)} - R_3^{-1}(\psi) \mathbf{p}_{n_j}) \right] \end{aligned} \quad (5.7)$$

where  $F_V^\circ$  are now Fourier integrals over a sharp sphere whose solution is known:

$$F_V^{(\circ)}(\mathbf{p}_{\rho(n)} - R_3^{-1}(\psi) \mathbf{p}_n) = \frac{1}{(2\pi)^3} \int_V d^3 \mathbf{x} e^{i(\mathbf{p}_{\rho(n)} - R_3^{-1}(\psi) \mathbf{p}_n) \cdot \mathbf{x}} = \frac{R^2}{2\pi^2} \frac{j_1(|\mathbf{p}_{\rho(n)} - R_3^{-1}(\psi) \mathbf{p}_n| R)}{|\mathbf{p}_{\rho(n)} - R_3^{-1}(\psi) \mathbf{p}_n|} \quad (5.8)$$

where  $R$  is the radius,  $j_1$  is the spherical Bessel function of the first kind and  $R_3(\psi)$  is a rotation of an angle  $\psi$  along the  $z$  axis.

The channel weight including parity, C-parity and isospin conservation, can be calculated introducing projectors in (4.7), (4.8) and the full projector onto an irreducible state of  $\text{IO}(1,3)^\uparrow$  in (4.10). Abelian charges conservation can be easily implemented algorithmically just by imposing that  $\sum_j^k \mathbf{q}_j N_j = \mathbf{Q}$ , where  $\mathbf{q}_j$  stands for the set of charges of the hadron species  $j$ .

In order to write the final result, one needs to first introduce the concept of *type* and *species* of particles: particles species differ by whatever quantum number whereas particles belong to the same type if they are light-flavoured mesons belonging to the same isospin multiplet or if they are particle-antiparticle pair. Thus, if  $N$  is the total number of particles in a channel  $\{N_j\} = (N_1, \dots, N_K)$ , we have:

$$N = \sum_{j=1}^k N_j = \sum_{j=1}^K L_j$$

$N_j$  being the multiplicity of species  $j$  and  $L_j$  the multiplicity of the type  $j$ ;  $k$  be the total number of species and  $K$  be total number of types.

If  $\Pi_f$  and  $\chi_C$  denote the product of all intrinsic parities and C-parities<sup>5</sup> of particles in the channel,  $S_j$  the spin of particles of type  $j$  and  $\rho_j$  a permutation of the integers  $1, \dots, L_j$ ,  $\chi(\rho_j)$  its

<sup>5</sup>Indeed, this factor includes additional charge conjugation phase factors of light-flavoured mesons [19].

parity and  $b_j = 0, 1$  for bosons and fermions respectively, the microcanonical channel weight reads:

$$\begin{aligned}
\Omega_{\{\rho_j\}} &= \sum_{\{\rho_j\}} \left[ \prod_{j=1}^K \chi(\rho_j)^{b_j} \right] \frac{1}{8\pi} \int_0^{4\pi} d\psi \left[ \prod_{j=1}^k \frac{1}{N_j!} \prod_{n_j=1}^{N_j} \int d^3 \mathbf{p}_{n_j} \right] \\
&\times \delta^4 \left( P - \sum_{n=1}^N p_n \right) \sin(\psi/2) \sin[(J+1/2)\psi] \prod_{j=1}^K \left[ \prod_{l_j=1}^{L_j} \left[ \frac{\sin[(S_j + \frac{1}{2})l_j\psi]}{\sin(\frac{l_j\psi}{2})} \right]^{h_{l_j}(\rho_j)} \right] \\
&\times \left( \prod_{j=1}^K \prod_{l_j=1}^{L_j} F_V^\circ(\mathbf{p}_{\rho_j(l_j)} - \mathbf{R}_3^{-1}(\psi)\mathbf{p}_{l_j}) + \prod_{j=1}^K \prod_{l_j=1}^{L_j} F_V^\circ(\mathbf{p}_{\rho_j(l_j)} + \mathbf{R}_3^{-1}(\psi)\mathbf{p}_{l_j}) \right) \\
&\times \left( \mathcal{J}_\rho^{\{N_j\}}(I, I_3) \prod_{j=1}^K \prod_{l_j=1}^{L_j} \delta_{\alpha_{\rho_j(l_j)} \alpha_{l_j}} + C\chi_C \bar{\mathcal{J}}_\rho^{\{N_j\}}(I, I_3) \prod_{j=1}^K \prod_{l_j=1}^{L_j} \delta_{-\alpha_{\rho_j(l_j)} \alpha_{l_j}} \right)
\end{aligned} \tag{5.9}$$

where  $h_{n_j}(\rho_j)$  is the number of cyclic permutation with  $l_j$  elements in  $\rho_j$  so that  $\sum_{l_j=1}^\infty l_j h_{l_j}(\rho_j) = N_j$  and where  $\alpha(l_j)$  is a set of quantum numbers (baryonic number and strangeness) of the  $l_j$ -th particle. The factors:

$$\begin{aligned}
\mathcal{J}_\rho^{\{N_j\}}(I, I_3) &\equiv \left[ \prod_{j=1}^K \langle I_j, \{I_3^{l_j}\} | \right] |I, I_3\rangle \langle I, I_3| \left[ \prod_{j=1}^K | \{I_j, I_3^{\rho_j(l_j)}\} \rangle \right] \\
\bar{\mathcal{J}}_\rho^{\{N_j\}}(I, I_3) &\equiv \left[ \prod_{j=1}^K \langle I_j, \{I_3^{l_j}\} | \right] |I, I_3\rangle \langle I, I_3| \left[ \prod_{j=1}^K | I_j, \{-I_3^{\rho_j(l_j)}\} \rangle \right]
\end{aligned} \tag{5.10}$$

are isospin coefficient. They have been calculated by using a recursive algorithm based on a tree-like coupling scheme [19].

## 6. Numerical evaluation

The channel weight in (5.9) cannot be evaluated analytically and is therefore necessary to resort to a numerical method. Whereas the sum over permutations can be performed by using well known algorithms and isospin coefficients can be evaluated by means of a recursive algorithm, the most difficult task is momentum integration, which has been performed by using the *importance sampling method*.

If we let  $f(x)$  be the function to integrate, the method consists in a random extraction<sup>6</sup> of the variables  $x$ , within the integration range, according to a certain probability density  $g(x)$ . In order to reduce the statistical error affecting the estimation, such distribution should meet the following requirements:

1. it must be as similar as possible to  $f(x)$ ,
2. it must be fast to sample,
3. it must be non-zero over the whole integration domain, otherwise the estimator would be biased.

<sup>6</sup>In numerical integrations based on this method one usually refers to pseudo-random numbers.

The integral of  $f(x)$  thus becomes (assuming  $g$  normalized to 1):

$$I = \int_a^b dx f(x) = \int_a^b dx \frac{f(x)}{g(x)} g(x) \doteq \frac{(b-a)}{N_s} \sum_{i=1}^{N_s} \frac{f(x_i)}{g(x_i)} \quad (6.1)$$

where  $x_i$  are random variables extracted according to the distribution  $g(x)$ . The expression of the variance  $\sigma_I^2$  on the estimator of  $I$  turns then out to be:

$$\sigma_I^2 = \langle I^2 \rangle - \langle I \rangle^2 = \frac{1}{N_s} \int g(x) dx \left( \frac{f(x)}{g(x)} \right)^2 - \frac{1}{N_s} \left( \int g(x) dx \frac{f(x)}{g(x)} \right)^2 \quad (6.2)$$

and it is minimized by the choice of a  $g(x)$  as similar as possible to  $f(x)$ . The advantages of this method are evident: with the same number of extractions one can obtain a smaller variance with respect to a flat distribution. Moreover if  $g(x)$  can be sampled sufficiently fast one can obtain a smaller variance in a shorter time, thus a more efficient algorithm.

Turning to Eq. (5.9), we develop the  $\delta^4$  factor of energy-momentum conservation as (in the cluster's rest frame):

$$\delta^4 \left( P - \sum_{n=1}^N p_n \right) = \delta \left( M - \sum_{n=1}^N \varepsilon_n \right) \delta^3 \left( \sum_{n=1}^N \mathbf{p}_n \right) \quad (6.3)$$

and set:

$$\mathbf{p}_N = - \sum_{n=1}^{N-1} \mathbf{p}_n. \quad (6.4)$$

After solving  $\delta \left( M - \sum_{n=1}^N \varepsilon_n \right)$  in terms of the modulus of the  $N-1$ -th particle momentum  $p_{N-1}$  we are thus left with  $3N-3$  variables:  $N-2$  moduli of particle momenta,  $N-1$  solid angles, 1 angle  $\psi$ .

We used a flat distributions for all angles, while particle kinetic energies (hence momenta) have been extracted according to a suitable auxiliary distribution which was used already in [23]. Such a distribution is the so called  $\beta$  function and reads:

$$\beta(x) = \frac{\Gamma(a+b)}{\Gamma(a)\Gamma(b)} x^{a-1} (1-x)^{b-1} \quad (6.5)$$

where  $a$  and  $b$  are two positive parameter and  $0 < x < 1$ . In our case the variable  $x$  is  $t/t_{\max}$ , where  $t_{\max}$  is the difference between the total energy of the system and the sum of all particle masses in the channel  $\{N_j\}$ , i.e. the total kinetic energy available. The expression (6.5) therefore reads:

$$\beta \left( \frac{t}{t_{\max}} \right) = \frac{\Gamma(a+b)}{\Gamma(a)\Gamma(b)} \left( \frac{t}{t_{\max}} \right)^{a-1} \left( 1 - \frac{t}{t_{\max}} \right)^{t_{\max}/T} \quad (6.6)$$

where we identified  $b-1 = t_{\max}/T$  and where  $T$  is the corresponding temperature in the canonical ensemble which can be obtained through a saddle point expansion [11, 12]. As has been shown in [23], a good choice for the parameter  $a$  is:

$$a-1 = \frac{1}{2} + \frac{3}{2} e^{-2m_j} \quad (6.7)$$

where we introduced an empirical dependence of  $a$  on the particle masses ( $m_j$  are expressed in GeV). This distribution is very close to the grand-canonical distribution of particle kinetic energies and it is fast to sample. The algorithm used to randomly extract particle kinetic energies according to the distribution  $\beta$  is the Cheng's BB algorithm [24] which samples variables through a very efficient rejection method.

As will be discussed in next section, we will account of interactions between strongly stable hadrons according to the hadron-resonance gas model, i.e. handling resonances as free particles. At this stage, the resonances mass broadening can be straightforwardly introduced by extracting masses at each step according to the relativistic Breit-Wigner distribution:

$$B_r(m) \equiv \frac{1}{2\pi} \frac{\Gamma_r}{(m - m_r)^2 + \Gamma_r^2/4} \quad (6.8)$$

where  $m_r$  is the average mass and  $\Gamma_r$  is the width.

## 7. Probability of exclusive channels

So far we have been dealing with the microcanonical partition function of the ideal hadron gas. There exists a very convenient way of writing the microcanonical partition function as the sum of the free microcanonical partition function plus an interaction term expressed in terms of the scattering matrix. This formula was obtained by Dashen, Ma and Bernstein[25] (DMB) in the late 60's and it is the theoretical basis of the so-called hadron-resonance gas model. In this model, stable hadrons with respect to strong interactions and resonances are treated on an equal footing as free particles, what turns out to be a very good approximation of an interacting hadron gas.

According to this theorem, the microcanonical partition function in the infinite volume limit is expressed as the sum of the free partition function plus a term involving the (reduced) scattering matrix  $\mathcal{S}$ :

$$\Omega = \sum_{h_V} \langle h_V | P_i | h_V \rangle \xrightarrow{V \rightarrow \infty} \text{tr} P_i = \text{tr} P_{0i} + \frac{1}{4\pi i} \text{tr} P_{0i} \mathcal{S}^{-1} \frac{\overleftrightarrow{\partial} \mathcal{S}}{\partial E} \quad (7.1)$$

where  $P_i$  and  $P_{0i}$  are respectively projectors involving the interacting and the free hamiltonian and where  $\Omega$  is expressed as a trace since the set of states  $|h_V\rangle$  is a full basis of the Hilbert space when  $V \rightarrow \infty$ . Unfortunately, if we retain a finite volume  $V$ , the DMB procedure does not produce an expression as simple as (7.1). One should therefore keep in mind that all applications of the hadron-resonance gas model stemming from (7.1) strictly hold in the limit of large volumes  $V \gtrsim 10 \text{ fm}^3$  [19].

In order to define a good probability for the interacting hadron gas, one could draw inspiration from the DMB theorem and *redefine* the probability of observing a final state  $|f\rangle$  as:

$$\rho_f \propto \langle f | P_{0i} P_V P_{0i} | f \rangle + \frac{1}{4\pi i} \langle f | P_{0i} \mathcal{S}^{-1} \frac{\overleftrightarrow{\partial} \mathcal{S}}{\partial E} P_V P_{0i} | f \rangle \quad (7.2)$$

where the rightmost term account for interactions. Accordingly, the microcanonical weight of a *final channel* with only strongly stable hadrons will be then obtained integrating Eq. (7.2) over particle momenta and helicities.

If we assume that the predominant contribution comes from resonating interactions, the interaction term in (7.2) can be calculated expanding the  $\mathcal{S}$  matrix in a cluster decomposition as a sum of digrams like these shown in fig. 2. If only symmetric diagrams (see e.g. first two diagrams

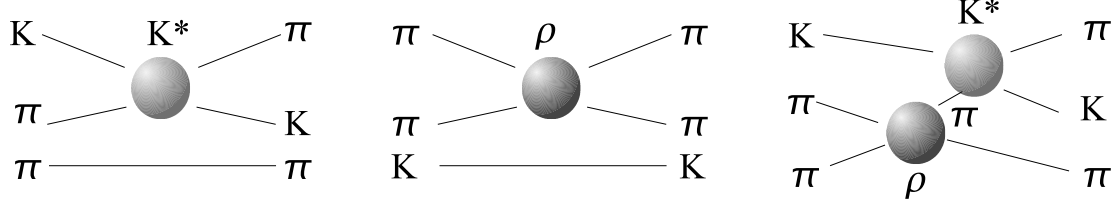


**Figure 2:** Three examples of diagrams which contribute to the probability of the channel  $K\pi\pi$  according to the Dashen-Ma-Bernstein theorem prescription. First two diagrams from left are symmetric while the rightmost one is non-symmetric.

from left in fig. 2) are retained in the DMB theorem expansion and interference of overlapping resonances is neglected, this is given by a weighted sum of free microcanonical weights (5.9) of channels including both hadrons and resonances (which can then be handled as free particles with distributed mass) eventually decaying into the final hadrons of the channel. We have thus recovered the usually known recipe of the hadron-resonance gas model.

Given a final channel  $\{N_j\}$ , one should find all possible *parent channels* whose hadrons and resonances decay into it. The search for all parent channels is a multi-step recursive problem in that many generations can be involved. If we denote by  $\{N_j\}_{(1)}$  a channel which can directly decay into the channel  $\{N_j\}$ , by  $\{N_j\}_{(2)}$  a channel which can directly decay in  $\{N_j\}_{(1)}$  and so on, one has to find all possible decay trees like those shown in Fig. (3). In view of the large number of resonances, this task is not a trivial one: a suitable algorithm has been devised for this purpose. The probability

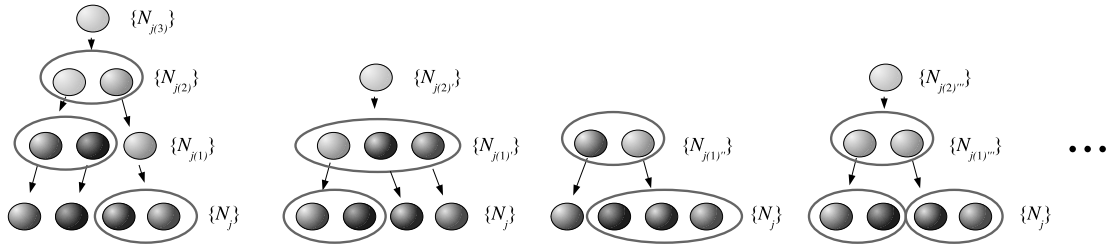


**Figure 3:** Examples of possible decay trees for a four particles channel. Circles encompass decay products of the particle at higher level.

$\rho_{\{N_j\}}$  of observing a final channel  $\{N_j\}$  can then be expressed as a finite sum:

$$\begin{aligned} \rho_{\{N_j\}} \propto \omega_{\{N_j\}} \equiv & \Omega_{\{N_j\}} + \text{BR}_{(1)}\Omega_{\{N_j\}_{(1)}} + \text{BR}_{(2)}\text{BR}^{(1)}\Omega_{\{N_j\}_{(2)}} + \dots \\ & + \text{BR}_{(1)'}\Omega_{\{N_j\}_{(1)'}} + \text{BR}^{(2)'}\text{BR}_{(1)'}\Omega_{\{N_j\}_{(2)'}} + \dots \end{aligned} \quad (7.3)$$

where  $\text{BR}_{(i)}$  is the product of branching ratios of particles in the channel  $\{N_j\}_{(i)}$  decaying into particles in the channel  $\{N_j\}_{(i-1)}$  and where  $\omega_{\{N_j\}}$  is the channel weight where contributions of parent channels are included.

It should be pointed out that there are more contributions to the microcanonical weight of a final channel which have been neglected. These stem from the non-symmetric diagrams (see the rightmost diagram in fig. 2) whose value depend on unknown parameters [19]. They have been neglected in this work.

### 7.1 Strangeness suppression factor

We allow deviations from statistical equilibrium of channels involving particles with strange valence quarks introducing a phenomenological parameter, the *strangeness suppression factor*  $\gamma_S$ . This parameter has been widely used in inclusive hadron multiplicity analyses and it is likely to be needed also in the analysis of exclusive rates at low energy. In order to have agreement with the  $\gamma_S$  definition in the canonical and grand-canonical limit, one should multiply the microcanonical weight of a channel by  $\gamma_S^{s_j}$   $s_j$  being the number of valence strange quarks of each particle:

$$\Omega_{\{N_j\}} \rightarrow \left[ \prod_{j=1}^k (\gamma_S^{s_j})^{N_j} \right] \Omega_{\{N_j\}}. \quad (7.4)$$

The  $\gamma_S$  factor also applies to neutral mesons with valence strange quarks like  $\eta$ ,  $\phi$  etc. Since the wavefunction of such particles is in general a superposition like  $C_u u\bar{u} + C_d d\bar{d} + C_s s\bar{s}$  with  $|C_u|^2 + |C_d|^2 + |C_s|^2 = 1$ , only the component  $s\bar{s}$  of the wavefunction is suppressed, i.e. we multiply by:

$$|C_s|^2 \gamma_S^2 + (1 - |C_s|^2).$$

We have used mixing angles quoted by the Particle Data Book [26].

### 7.2 Single resonance contribution

According to DMB theorem, the microcanonical partition function of an interacting hadron gas also gets non-vanishing contribution from diagrams with a single resonance  $r$ . This reads:

$$\Omega_r = \frac{V}{(2\pi)^3} B_r(M) \quad (7.5)$$

where  $V$  is the volume and  $B_r(M)$  is a normalized Breit-Wigner distribution:

$$B_r(M) \equiv \frac{1}{2\pi} \frac{\Gamma_r}{(M - M_r)^2 + \Gamma_r^2/4}. \quad (7.6)$$

In terms of the diagrammatic description with the decay tree in fig. (3), this correspond to the highest ancestor of the channel, with a single resonance having the same quantum numbers of the cluster itself. The contribution (7.5) is globally suppressed by a factor  $\sim 1/(M - M_r)^2 + \Gamma_r^2/4$  or smaller, so that for cluster masses sufficiently larger than the difference  $M_r - \Gamma_r$ , this is expected to become negligible. Small as it can be, though, the single- resonance term (including multiple resonance interference) cannot be excluded in principle from the calculation of the microcanonical partition function. However, in our formulation of the statistical model the starting point is an assumed probability given by a DMB theorem-inspired formula (7.2) and the single resonance contribution may be well excluded by hand.

## 8. An analysis of $e^+e^-$ collisions at low energy

There have been several attempts to reproduce hadron multiplicities and some multi-pion(kaon) differential cross sections in low energy  $e^+e^-$  collisions [15] by using statistical-thermodynamical or statistical-inspired models in the past. Yet, to simplify numerical calculations, none of them properly took into account the full set of conservation laws, which is a clear drawback because in few body decays all of them are indispensable. Now, we are in a position to make a thorough test of the statistical *ansatz* in a more rigorous formulation, taking into account properly conserved quantities and the finite volume of the hadron-emitting source.

According to the discussion in sec. (3), we will assume the formation of a single cluster at rest whose mass coincide with  $\sqrt{s}$  and other quantum numbers will be given by the initial colliding particles. In low energy  $e^+e^-$  collision, the hadron production is dominated by the diagram with an intermediate virtual photon (see the pictorial sketch in fig. 4), so that the hadronizing cluster has spin, parity and C-parity assignment  $J^{PC} = 1^{--}$ . On the other hand, initial isospin is unknown; in the Vector Dominance Model (VDM) this depends on the coupling of the photon to different resonances, but we will be working in a mass region above 2 GeV quite far from resonance region. Therefore, we will assume an unknown statistical mixture of  $I = 0$  and  $I = 1$  initial state disregarding interference terms and introducing a free parameter  $f_1$ , the fraction of  $I = 1$  state:

$$f_1|1,0\rangle\langle 1,0| + (1-f_1)|0,0\rangle\langle 0,0|.$$

where isospin states have been denoted as  $|I, I_3\rangle$ . In order to completely define the cluster, besides his mass, we must fix his volume. We thus introduce the energy density parameter  $\rho$ :

$$\rho \equiv \frac{M}{V} = \frac{3M}{4\pi R^3} \quad (8.1)$$

where  $M$  is the mass.

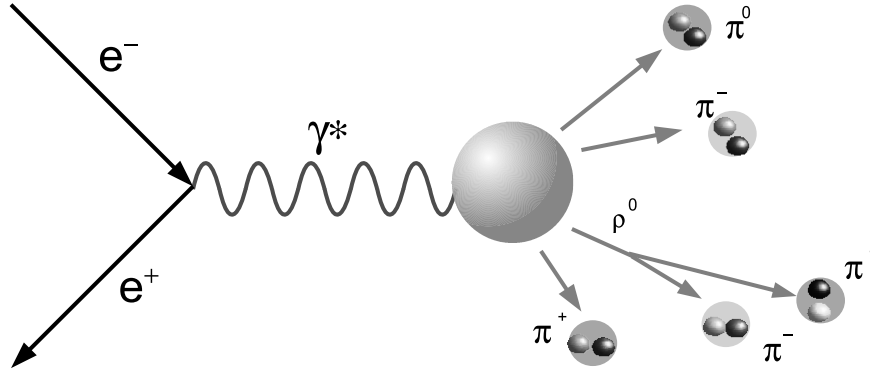


**Figure 4:** Pictorial representation of a low energy  $e^+e^-$  collision with formation of a single cluster.

We want to compare the predictions of the SHM with measured production rates of several exclusive channels. A relevant problem in this comparison is how to deal with the contribution of single resonances. There are two main options in this regard:

1. Exclude single-resonance contribution (7.5) from the model formulation.
2. Include single-resonance contribution in the model formulation.

The option 1 requires a subtraction of the contribution of single resonances to the measured cross section of a given exclusive channel and the comparison with  $\Omega^{(>1)}$  microcanonical weight of the channel, where ( $> 1$ ) just indicates that single-resonance contribution is excluded. This is a clearly difficult task because we have a poor knowledge of the widths, branching ratios and the widths in  $e^+e^-$  of the whole set of  $J^{PC} = 1^{--}$  resonances, which are needed for the subtraction. We also ignore interference phases of these resonances. On the other hand, the option 2 does not require any cross-section subtraction and, albeit resonance interference is still not taken into account and many experimental resonance branching ratios are poorly known, we are not required to know the  $\Gamma(r \rightarrow e^+e^-)$ ; we just compare the model outcome with the *relative* yields of measured channels.

In both cases, though, it is advantageous to be sufficiently far from the resonance region to minimize the impact of poor knowledge of hadronic resonance characteristics. Furthermore, we do not want to get over the charm production threshold and this constrains our interval to the energy range 2-3 GeV. Sufficiently many experimental measurements can be found in this range in literature for  $\sqrt{s} = 2.1$  GeV and  $\sqrt{s} = 2.4$  GeV and this is what we have analyzed. Indeed, we will see that at such energy points, known  $1^{--}$  resonances contribute (in the incoherent sum approximation) at most 10% to two-body channels.

To compare SHM predictions with measured cross sections, we have used branching ratios quoted by the Particle Data Book [26] to calculate  $\omega_{\{N_j\}}$  in (7.3). A dimensional factor  $A(\sqrt{s})$  is introduced:

$$\sigma_{\{N_j\}} \longrightarrow A(\sqrt{s})\omega_{\{N_j\}}. \quad (8.2)$$

(where  $\sigma_{\{N_j\}} \equiv \sigma(e^+e^- \rightarrow \{N_j\})$ ) which is determined, at a given energy  $\sqrt{s}$ , through the minimization of the  $\chi^2$ :

$$\chi^2 \equiv \sum_{\{N_j\}_{\text{meas.}}} \frac{(\sigma_{\{N_j\}} - A\omega_{\{N_j\}})^2}{\Delta_{\sigma_{\{N_j\}}}^2 + A^2\Delta_{\omega_{\{N_j\}}}^2}. \quad (8.3)$$

The above sum runs over measured channels;  $\Delta_{\sigma_{\{N_j\}}}$  and  $\Delta_{\omega_{\{N_j\}}}$  are the uncertainties on measured cross sections and on channel weight evaluated with the model respectively. The latter is essentially the sum of the statistical error (owing to the finite number of sampling in Monte-Carlo integration) and the systematic uncertainty in the branching ratios of resonances in Eq. (7.3). We have estimated the systematic uncertainty by varying the branching ratios by their errors quoted by the Particle Data Book or by making an educated guess of these errors.

The comparison with experimental data is shown in tab. (1) and (2) at  $\sqrt{s} = 2.1$  GeV and  $\sqrt{s} = 2.4$  GeV respectively. We have performed a coarse scan in energy density, and the two parameters  $f_1$  and  $\gamma_S$  of the branching ratios. In the table, the results obtained at four energy density values (0.1, 0.5, 1.0, 1.5 GeV/fm<sup>3</sup>) and the best values of  $f_1$  and  $\gamma_S$  are shown.

As it can be seen, the dependence on energy density is not very strong and the best values (in boldface on tables) vary from  $\rho = 0.1$  GeV/fm<sup>3</sup> in tab. (1) and  $\rho = 1.5$  GeV/fm<sup>3</sup> in tab. (2). For

$\sqrt{s} = 2.4 \text{ GeV}/\text{fm}^3$  the best value of  $\gamma_S$  is 1.4. This is quite unusual in statistical models where (at least at high energies)  $\gamma_S \leq 1$ .

In both cases the agreement is fair and for  $\sqrt{s} = 2.4 \text{ GeV}$  model predictions are closer to data. This is also due to the smaller number of listed exclusive channels which, in turn, implies a better fitting of normalizing constant  $A$ .

At best values of parameters, single resonance channels are important for  $\pi^+\pi^- \sim 12\%$  and  $\pi^+\pi^-\pi^0$  ( $\sim 3.5\%$ ) at  $\sqrt{s} = 2.1 \text{ GeV}$  and for  $\pi^+\pi^-\pi^0$  ( $\sim 7\%$ ) for  $\sqrt{s} = 2.4 \text{ GeV}$ . This value is higher than at  $\sqrt{s} = 2.1 \text{ GeV}$  because, even if tails of overlapping resonances are lower (the main contribution comes from  $\omega(1650)$ ), at higher energy densities few-particles channels have higher statistical weight.

In tab. (1), the channel  $\eta\pi^+\pi^-$  is overestimated by the model for all energy density values and in tab. (2) the same happens for  $\omega\pi^+\pi^-$ . This might owe to our assumption of a mixture of isospin states (instead of a superposition) for the initial photon state and a too simple parametrization of strangeness suppression. This could be also the reason for  $\gamma_S = 1.4$  at  $\sqrt{s} = 2.4 \text{ GeV}$ . Probably, a better agreement might be achieved enforcing the full flavour symmetry group SU(3) and correcting for the explicit flavour-breaking. It should also be reminded that we describe interactions by using DMB theorem which strictly holds for large volumes so that deviations may well arise at volumes  $21 \text{ fm}^3$  corresponding to the best density in tab. (1) and even more at the volume of  $1.4 \text{ fm}^3$  corresponding to  $\rho = 1.5 \text{ GeV}/\text{fm}^3$  in tab. (2).

Other approximations which may affect results are the absence of resonance interference between overlapping resonances, the exclusion of further terms in the DMB diagrammatic expansion and the very fact that we kept only the resonant part of the interaction. In inclusive quantities, these effects probably wash out when summing over many final channels but this may not be the case for some specific few-body exclusive channels.

channel	$\sigma$ (nb) (model)				$\sigma$ (nb) (exp.)	References
	$\rho = 0.1 \text{ GeV}/\text{fm}^3$ $f_1 = 0.9 \ \gamma_S = 1.0$	$\rho = 0.5 \text{ GeV}/\text{fm}^3$ $f_1 = 0.9 \ \gamma_S = 1.2$	$\rho = 1.0 \text{ GeV}/\text{fm}^3$ $f_1 = 0.9 \ \gamma_S = 1.2$	$\rho = 1.5 \text{ GeV}/\text{fm}^3$ $f_1 = 0.9 \ \gamma_S = 1.2$		
$\pi^+ \pi^-$	$0.25 \pm 0.004 \pm 0.02$	$0.49 \pm 0.004 \pm 0.06$	$0.6 \pm 0.004 \pm 0.1$	$0.7 \pm 0.004 \pm 0.1$	$0.35 \pm 0.17$	[27]
$\pi^+ \pi^- \pi^0$	$0.07 \pm 0.005 \pm 0.01$	$0.09 \pm 0.0005 \pm 0.02$	$0.1 \pm 0.0004 \pm 0.02$	$0.1 \pm 0.0003 \pm 0.02$	$0.398 \pm 0.099$	[28, 29, 30, 31]
$\pi^+ \pi^- \pi^0 \pi^0$	$6.6 \pm 0.1 \pm 0.5$	$3.8 \pm 0.02 \pm 0.4$	$3.4 \pm 0.01 \pm 0.4$	$3.2 \pm 0.01 \pm 0.3$	$15.8 \pm 3.4$	[31]
$\pi^+ \pi^- \pi^+ \pi^-$	$5.4 \pm 0.1 \pm 0.5$	$3.3 \pm 0.02 \pm 0.4$	$2.9 \pm 0.01 \pm 0.4$	$2.7 \pm 0.006 \pm 0.4$	$5.142 \pm 0.263$	[32, 33, 34]
$\pi^+ \pi^- \pi^+ \pi^- \pi^0$	$1.46 \pm 0.02 \pm 0.07$	$0.92 \pm 0.004 \pm 0.07$	$0.81 \pm 0.003 \pm 0.06$	$0.73 \pm 0.002 \pm 0.05$	$2.5 \pm 2.4$	[31]
$p\bar{p}$	$0.468 \pm 0.002 \pm 0$	$0.662 \pm 0.002 \pm 0$	$0.744 \pm 0.002 \pm 0$	$0.763 \pm 0.002 \pm 0$	$0.571 \pm 0.068$	[35, 36, 37, 38]
$n\bar{n}$	$0.473 \pm 0.002 \pm 0$	$0.662 \pm 0.002 \pm 0$	$0.745 \pm 0.002 \pm 0$	$0.764 \pm 0.002 \pm 0$	$0.95 \pm 0.23$	[35, 39]
$K^+ K^- \pi^+ \pi^- \pi^+ \pi^-$	$0.0381 \pm 0.0003 \pm 0.0002$	$0.00113 (\pm 0.7 \pm 1) 10^{-5}$	$0.000195 (\pm 1 \pm 3) 10^{-6}$	$6.8 10^{-5} (\pm 0.7 \pm 2) 10^{-6}$	$0.015 \pm 0.015$	[40]
$K^+ K^- \pi^+ \pi^-$	$3.4 \pm 0.04 \pm 0.1$	$3.39 \pm 0.01 \pm 0.07$	$2.84 \pm 0.01 \pm 0.05$	$2.53 \pm 0.006 \pm 0.05$	$3.5 \pm 0.27$	[34, 41]
$\eta \pi^+ \pi^-$	$1.2 \pm 0.03 \pm 0.2$	$1.5 \pm 0.01 \pm 0.2$	$1.5 \pm 0.01 \pm 0.2$	$1.4 \pm 0.01 \pm 0.1$	$0.22 \pm 0.16$	[42]
$\omega \pi^+ \pi^-$	$0.285 \pm 0.004 \pm 0.001$	$0.234 \pm 0.001 \pm 0.002$	$0.225 \pm 0.001 \pm 0.004$	$0.216 \pm 0.0006 \pm 0.005$	$0.27 \pm 0.12$	[29]

**Table 1:** Exclusive cross sections in  $e^+e^-$  collisions at  $\sqrt{s} = 2.1$  GeV. The first error on model calculations is statistical and the second is the uncertainty due to poorly known resonance branching ratios. The energy density value in best agreement with data is in boldface. Quoted experimental data are weighted averages of measures in references.

channel	$\sigma$ (nb) (model)				$\sigma$ (nb) (exp.)	References
	$\rho = 0.1 \text{ GeV}/\text{fm}^3$ $f_1 = 0.5 \ \gamma_S = 0.8$	$\rho = 0.5 \text{ GeV}/\text{fm}^3$ $f_1 = 0.3 \ \gamma_S = 1.4$	$\rho = 1.0 \text{ GeV}/\text{fm}^3$ $f_1 = 0.3 \ \gamma_S = 1.4$	$\rho = 1.5 \text{ GeV}/\text{fm}^3$ $f_1 = 0.3 \ \gamma_S = 1.4$		
$\pi^+ \pi^- \pi^0$	$0.12 \pm 0.004 \pm 0.02$	$0.17 \pm 0.001 \pm 0.04$	$0.2 \pm 0.001 \pm 0.05$	$0.21 \pm 0.001 \pm 0.05$	$0.254 \pm 0.071$	[30, 29]
$\pi^+ \pi^- \pi^+ \pi^-$	$1.6 \pm 0.02 \pm 0.2$	$0.9 \pm 0.004 \pm 0.3$	$0.9 \pm 0.002 \pm 0.3$	$0.8 \pm 0.002 \pm 0.3$	$1.3 \pm 0.38$	[43]
$p\bar{p}$	$0.101 \pm 0.001 \pm 0$	$0.165 \pm 0.001 \pm 0$	$0.215 \pm 0.001 \pm 0$	$0.233 \pm 0.001 \pm 0$	$0.31 \pm 0.12$	[44, 45]
$n\bar{n}$	$0.102 \pm 0.001 \pm 0$	$0.165 \pm 0.001 \pm 0$	$0.213 \pm 0.001 \pm 0$	$0.234 \pm 0.001 \pm 0$	$0.69 \pm 0.29$	[35]
$K^+ K^- \pi^+ \pi^- \pi^+ \pi^-$	$0.208 \pm 0.002 \pm 0.002$	$0.288 \pm 0.001 \pm 0.003$	$0.256 \pm 0.001 \pm 0.002$	$0.245 \pm 0.001 \pm 0.002$	$0.295 \pm 0.075$	[40]
$\eta \pi^+ \pi^-$	$0.17 \pm 0.008 \pm 0.04$	$0.28 \pm 0.004 \pm 0.065$	$0.3 \pm 0.002 \pm 0.07$	$0.301 \pm 0.002 \pm 0.07$	$0.22 \pm 0.11$	[42]
$\omega \pi^+ \pi^-$	$0.62 \pm 0.008 \pm 0.04$	$1.5 \pm 0.006 \pm 0.5$	$1.6 \pm 0.004 \pm 0.6$	$1.6 \pm 0.004 \pm 0.6$	$0.24 \pm 0.19$	[29]

**Table 2:** Exclusive cross sections in  $e^+e^-$  collisions at  $\sqrt{s} = 2.4 \text{ GeV}$ . The first error on model calculations is statistical and the second is the uncertainty due to poorly known resonance branching ratios. The energy density value in best agreement with data is in boldface. Quoted experimental data are weighted averages of measures in references.

## 9. Resonances as hadronizing clusters

The identification of (heavy) resonances with extended clusters is a tempting conceptual step. Hagedorn first put forward this idea in the '60s [8] laying the foundations of the Statistical Bootstrap Model. Also the MIT Bag model conceives resonances and hadrons as extended massive objects from the very beginning, giving rise to many physical consequences. It is therefore a natural step to make the same identification in the framework of the statistical hadronization model and check, on the basis of existing measurements, whether at least heavier resonances decay statistically into multi-hadronic channels. If this turned out to be the case, we would achieve a major confirmation of the old Hagedorn idea that resonances are in turn made of resonances and hadrons.

We compared the branching ratios of heavy resonances with statistical model predictions. Theoretical branching ratios have been normalized by means of an external constant  $A$ :

$$BR(r \rightarrow \{N_j\}) \longrightarrow A \omega_{\{N_j\}}^{(>1)} \quad (9.1)$$

and not by calculating all possible decay channels. This is a drawback of present calculation which should be fixed in the near future. In (9.1),  $\omega_{\{N_j\}}^{(>1)}$  stands for the probability in (7.3) where only channels with at least two particles are included. As for  $e^+e^-$  collisions, branching ratios in Eq. (7.3) have been introduced as external inputs from [26].

In tables: (3),(4),(5),(6),(7) and (8) model predictions are compared with branching ratios of 6 heavy resonances (quoted by the Particle Data Book [46]):  $K_2^*(1430)$ ;  $\Lambda(1520)$ ;  $\pi_2(1670)$ ;  $\rho_3(1690)$ ;  $K_3^*(1780)$ ;  $K_4^*(2045)$ .

$K_2^*(1430)$					
channel	B.R. (model)				B.R. (exp.)
	$\rho = 0.02 \text{ GeV}/\text{fm}^3$ $\gamma_S = 1.0$	$\rho = 0.5 \text{ GeV}/\text{fm}^3$ $\gamma_S = 1.0$	$\rho = 0.6 \text{ GeV}/\text{fm}^3$ $\gamma_S = 1.0$	$\rho = 1.5 \text{ GeV}/\text{fm}^3$ $\gamma_S = 1.0$	
$K\pi$	$10.5 \pm 0.2 \pm 0$	$51.5 \pm 0.5 \pm 0$	$53.2 \pm 0.6 \pm 0$	$68.3 \pm 1.6 \pm 0$	$49.9 \pm 1.2$
$K^*(892)\pi$	$11.5 \pm 0.2 \pm 0$	$21.1 \pm 0.6 \pm 0$	$20.4 \pm 0.6 \pm 0$	$16 \pm 1.7 \pm 0$	$24.7 \pm 1.5$
$K^*(892)\pi\pi$	$51 \pm 1 \pm 0$	$5.4 \pm 0.1 \pm 0$	$4.75 \pm 0.08 \pm 0$	$3.2 \pm 0.05 \pm 0$	$13.4 \pm 2.2$
$K\rho$	$12.3 \pm 0.2 \pm 0$	$12.3 \pm 0.6 \pm 0$	$12.1 \pm 0.7 \pm 0$	$7.2 \pm 1.6 \pm 0$	$8.7 \pm 0.8$
$K\omega$	$14.3 \pm 0.2 \pm 0$	$9.4 \pm 0.7 \pm 0$	$9.1 \pm 0.8 \pm 0$	$4.8 \pm 1.7 \pm 0$	$2.9 \pm 0.8$

**Table 3:** Branching ratios of  $K_2^*(1430)$ . The first error on model calculations is statistical and the second is the uncertainty due to poorly known resonance branching ratios. The energy density value in best agreement with data is in boldface. The reference for quoted experimental data is [46].

We found parameters  $\rho$  and  $\gamma_S$  in best agreement with data (in boldface on tables) by trial and error and we also quote results for different values of the energy density, from 0.02 to 1.5  $\text{GeV}/\text{fm}^3$ . For each value of  $\rho$ ,  $\gamma_S$  has been chosen in order to get the best agreement with the data. Measured branching ratios are those quoted by the Particle Data Book [46].

There is a fair agreement of model and data even though large discrepancies appear for some channels like, for instance,  $\pi_2 \rightarrow \omega\rho$ . This channel has been excluded from the calculation of  $A$  because overestimated by the model.

It is interesting to look at the dependence on the energy density, especially comparing to the others the point  $\rho = 0.02 \text{ GeV}/\text{fm}^3$  in tables (3) and (4) of resonances  $K_2^*(1430)$  and  $\Lambda(1520)$ . It is interesting to note that the ratio between channels  $\Sigma\pi\pi$  and  $\Sigma\pi$  of  $\Lambda(1520)$  increases with

$\Lambda(1520)$					
channel	B.R. (model)				B.R. (exp.)
	$\rho = 0.02 \text{ GeV}/\text{fm}^3$ $\gamma_S = 1.0$	$\rho = 0.1 \text{ GeV}/\text{fm}^3$ $\gamma_S = 1.0$	$\rho = 0.5 \text{ GeV}/\text{fm}^3$ $\gamma_S = 1.0$	$\rho = 1.5 \text{ GeV}/\text{fm}^3$ $\gamma_S = 1.0$	
$N\bar{K}$	$42.3 \pm 0.4 \pm 0$	$40.1 \pm 1.1 \pm 0$	$20.2 \pm 5.7 \pm 0$	$5.5 \pm 12.1 \pm 0$	$45 \pm 1$
$\Sigma\pi$	$29.4 \pm 0.3 \pm 0$	$36.5 \pm 0.7 \pm 0$	$28.5 \pm 3.9 \pm 0$	$7.3 \pm 8.8 \pm 0$	$42 \pm 1$
$\Lambda\pi\pi$	$23.7 \pm 0.4 \pm 0$	$19.3 \pm 0.1 \pm 0$	$43.4 \pm 0.2 \pm 0$	$74.9 \pm 0.3 \pm 0$	$10 \pm 1$
$\Sigma\pi\pi$	$2.47 \pm 0.01 \pm 0$	$2.065 \pm 0.007 \pm 0$	$5.7 \pm 0.02 \pm 0$	$10.14 \pm 0.04 \pm 0$	$0.9 \pm 0.1$

**Table 4:** Branching ratios of  $\Lambda(1520)$ . The first error on model calculations is statistical and the second is the uncertainty due to poorly known resonance branching ratios. The energy density value in best agreement with data is in boldface. The reference for quoted experimental data is [46].

$\pi_2(1670)$					
channel	B.R. (model)				B.R. (exp.)
	$\rho = 0.02 \text{ GeV}/\text{fm}^3$ $\gamma_S = 0.6$	$\rho = 0.1 \text{ GeV}/\text{fm}^3$ $\gamma_S = 0.6$	$\rho = 0.5 \text{ GeV}/\text{fm}^3$ $\gamma_S = 0.6$	$\rho = 1.5 \text{ GeV}/\text{fm}^3$ $\gamma_S = 0.6$	
$f_2(1270)\pi$	$50 \pm 0.3 \pm 0$	$46.3 \pm 0.2 \pm 0$	$46.9 \pm 0.1 \pm 0$	$51 \pm 0.1 \pm 0$	$56.2 \pm 3.2$
$\rho\pi$	$35.6 \pm 0.4 \pm 0$	$39.7 \pm 0.3 \pm 0$	$40.1 \pm 0.2 \pm 0$	$37.2 \pm 0.2 \pm 0$	$31 \pm 4$
$\kappa\bar{K}^*(892) + \text{cc}$	$5.73 \pm 0.05 \pm 0$	$5.37 \pm 0.03 \pm 0$	$4.31 \pm 0.03 \pm 0$	$3.18 \pm 0.02 \pm 0$	$4.2 \pm 1.4$
$\omega\rho$ (Exclud.)	$76.3 \pm 0.7 \pm 0$	$62.9 \pm 0.5 \pm 0$	$43.8 \pm 0.3 \pm 0$	$29.7 \pm 0.2 \pm 0$	$2.7 \pm 1.1$

**Table 5:** Branching ratios of  $\pi_2(1670)$ . The normalization constant has been calculated excluding the channel  $\omega\rho$ . The first error on model calculations is statistical and the second is the uncertainty due to poorly known resonance branching ratios. The energy density value in best agreement with data is in boldface. The reference for quoted experimental data is [46].

$\rho_3(1690)$					
channel	B.R. (model)				B.R. (exp.)
	$\rho = 0.02 \text{ GeV}/\text{fm}^3$ $\gamma_S = 1.8$	$\rho = 0.3 \text{ GeV}/\text{fm}^3$ $\gamma_S = 0.6$	$\rho = 0.5 \text{ GeV}/\text{fm}^3$ $\gamma_S = 0.6$	$\rho = 1.5 \text{ GeV}/\text{fm}^3$ $\gamma_S = 0.4$	
$\pi\pi\pi\pi$	$59.7 \pm 2.4 \pm 0.02$	$70.9 \pm 1.2 \pm 0.1$	$60.5 \pm 1.1 \pm 0.1$	$46 \pm 2.1 \pm 0.02$	$71.1 \pm 1.9$
$\omega\pi$	$0.61 \pm 0.02 \pm 0$	$18.7 \pm 0.4 \pm 0$	$21 \pm 0.5 \pm 0$	$20.6 \pm 1.5 \pm 0$	$16 \pm 6$
$K\bar{K}\pi$	$48.8 \pm 12.2 \pm 0.0002$	$2.4 \pm 0.1 \pm 0.02$	$2 \pm 0.1 \pm 0.0005$	$0.9 \pm 0.2 \pm 0.1$	$3.8 \pm 1.2$
$K\bar{K}$	$3.18 \pm 0.06 \pm 0$	$1.25 \pm 0.02 \pm 0$	$1.5 \pm 0.03 \pm 0$	$0.33 \pm 0.02 \pm 0$	$1.58 \pm 0.26$
$\pi\pi$	$3.74 \pm 0.08 \pm 0$	$22.8 \pm 0.3 \pm 0$	$31 \pm 0.5 \pm 0$	$48.2 \pm 1.4 \pm 0$	$23.6 \pm 1.3$

**Table 6:** Branching ratios of  $\rho_3(1690)$ . The first error on model calculations is statistical and the second is the uncertainty due to poorly known resonance branching ratios. The energy density value in best agreement with data is in boldface. The reference for quoted experimental data is [46].

the energy density contrarily to expectations. This is due to the fact that the channel  $\Sigma^+\pi^-\pi^0$  is dominated by the parent channel  $\Sigma^0(1385)\pi^0$  which is produced substantially at rest and has a large statistical weight. Also in this case, as for  $e^+e^-$ , channels with  $\omega$  meson seem to be peculiar for some resonances like  $\pi_2(1670)$ . For  $K_3^*(1780)$  the best value of  $\gamma_S$  is slightly larger than 1.

Even though we have a fair agreement, it is still very difficult to draw a definite conclusion. It is important, as a next step, to improve this comparison without introducing any external normalization constant exploring all allowed final channels and studying more carefully the effect of turning on and off each conservation law to understand the main driving forces of the obtained values.

$K_3^*(1780)$					
channel	B.R. (model)				B.R. (exp.)
	$\rho = 0.02 \text{ GeV}/\text{fm}^3$ $\gamma_S = 1.2$	$\rho = 0.1 \text{ GeV}/\text{fm}^3$ $\gamma_S = 1.4$	$\rho = 0.5 \text{ GeV}/\text{fm}^3$ $\gamma_S = 1.6$	$\rho = 1.5 \text{ GeV}/\text{fm}^3$ $\gamma_S = 1.8$	
$K\rho$	$25.4 \pm 0.6 \pm 0$	$19.4 \pm 0.4 \pm 0$	$11.9 \pm 0.4 \pm 0$	$6.4 \pm 0.7 \pm 0$	$31 \pm 9$
$K^*(892)\pi$	$21.5 \pm 0.6 \pm 0$	$19.3 \pm 0.4 \pm 0$	$14 \pm 0.4 \pm 0$	$9.1 \pm 0.7 \pm 0$	$20 \pm 5$
$K\pi$	$19.9 \pm 0.5 \pm 0$	$18.8 \pm 0.3 \pm 0$	$19.8 \pm 0.3 \pm 0$	$20.5 \pm 0.6 \pm 0$	$18.8 \pm 1$
$K\eta$	$32.9 \pm 0.7 \pm 0$	$42.3 \pm 0.6 \pm 0$	$54.1 \pm 0.9 \pm 0$	$63.7 \pm 2.5 \pm 0$	$30 \pm 13$

**Table 7:** Branching ratios of  $K_3^*(1780)$ . The first error on model calculations is statistical and the second is the uncertainty due to poorly known resonance branching ratios. The energy density value in best agreement with data is in boldface. The reference for quoted experimental data is [46].

$K_4^*(2045)$					
channel	B.R. (model)				B.R. (exp.)
	$\rho = 0.02 \text{ GeV}/\text{fm}^3$ $\gamma_S = 1.2$	$\rho = 0.1 \text{ GeV}/\text{fm}^3$ $\gamma_S = 1.0$	$\rho = 0.5 \text{ GeV}/\text{fm}^3$ $\gamma_S = 1.0$	$\rho = 1.5 \text{ GeV}/\text{fm}^3$ $\gamma_S = 0.8$	
$K\pi$	$0.055 \pm 0.002 \pm 0$	$0.429 \pm 0.006 \pm 0$	$1.99 \pm 0.03 \pm 0$	$3.3 \pm 0.1 \pm 0$	$9.9 \pm 1.2$
$K^*(892)\pi\pi$	$4.7 \pm 0.1 \pm 0.03$	$8.3 \pm 0.1 \pm 0.1$	$8.3 \pm 0.1 \pm 0.2$	$7.6 \pm 0.3 \pm 0.2$	$9 \pm 5$
$K^*(892)\pi\pi\pi$	$20.5 \pm 1.1 \pm 0.1$	$9.6 \pm 0.2 \pm 0.1$	$7 \pm 0.1 \pm 0.07$	$8.4 \pm 0.4 \pm 0.06$	$7 \pm 5$
$K\rho\pi$	$7.3 \pm 1.4 \pm 0.02$	$12 \pm 0.5 \pm 0.06$	$10.9 \pm 0.4 \pm 0.08$	$9.6 \pm 0.5 \pm 0.09$	$5.7 \pm 3.2$
$K\omega\pi$	$3.5 \pm 0.2 \pm 0.0002$	$6.6 \pm 0.2 \pm 0.001$	$7.7 \pm 0.1 \pm 0.001$	$9.6 \pm 0.4 \pm 0.0002$	$5 \pm 3$
$K\phi\pi$	$4.1 \pm 0.4 \pm 0$	$2.67 \pm 0.09 \pm 0$	$2.6 \pm 0.09 \pm 0$	$1.2 \pm 0.1 \pm 0$	$2.8 \pm 1.4$
$K^*(892)\phi$	$0.635 \pm 0.008 \pm 0$	$1.18 \pm 0.01 \pm 0$	$2.25 \pm 0.05 \pm 0$	$1.1 \pm 0.1 \pm 0$	$1.4 \pm 0.7$

**Table 8:** Branching ratios of  $K_4^*(2045)$ . The first error on model calculations is statistical and the second is the uncertainty due to poorly known resonance branching ratios. The energy density value in best agreement with data is in boldface. The reference for quoted experimental data is [46].

## 10. Conclusions and Outlook

This work is the starting point of a new series of analyses of the statistical hadronization model (SHM) aiming to settle a long-standing debate [4, 5, 6, 7] on the interpretation of statistical-thermodynamical behaviour exhibited by particle multiplicities and transverse momentum spectra in high energy collisions. The comparison of the model with more observables, especially focusing on those which are more sensitive to peculiar features of the SHM, should allow us to distinguish between a genuine statistical equilibrium, i.e. hadrons are born at equilibrium within a finite volume (the SHM ansatz), and other non-statistical hypotheses which ascribe the “apparent” statistical equilibrium to a special property of the quantum dynamics governing hadronization (phase space dominance [6]). As was proposed in ref. [9], we started analyzing production rates of exclusive channels, which were indicated therein, in this sense, as much more effective observables with respect to inclusive quantities like average multiplicities. Unfortunately, for practical reasons, such quantities can be measured only in low energy (some GeV) collisions, where none of the conservation laws (including angular momentum, isospin, parity conservation) can be neglected.

We thus gave a formulation of the SHM in its fundamental microcanonical framework, enforcing the maximal set of conservation laws relevant to strong interaction and space-time symmetries by using the projector onto irreducible states of the orthochronous Poincaré group  $\text{IO}(1,3)^\dagger$  and fixing isospin, abelian charges, and C-parity (when the initial state is neutral). We defined the

probability to observe an asymptotic channel, i.e. a multihadronic state with fixed particle multiplicities, as a cluster's decay product, without invoking any large volume approximation. The *microcanonical channel weight* (proportional to the probability) has been calculated identifying confined states within the hadron emitting source (the cluster) as free states of the quantum field vanishing out of the cluster volume, thus achieving a microcanonical field theory; the corresponding microcanonical partition function being the sum over all channel of the channel weight. We took into account interactions among hadrons handling resonances as free particles, i.e. assuming the hadron-resonance gas model, that is a derivation of the more general Dashen-Ma-Bernstein theorem in the thermodynamical limit provided interference terms between nearby overlapping resonances and non-resonant interactions terms are neglected.

The channel weight has been calculated by using a purposely designed numerical method based on a Monte-Carlo integration which is the state of the art of microcanonical calculations for the hadron gas.

We made a preliminary test of the statistical hadronization model on production rates of exclusive channels in  $e^+e^-$  collisions at low energy, at two different values of  $\sqrt{s}$ : 2.1 GeV and 2.4 GeV. The calculation of required the inclusion of all conservation laws.

The obtained results are in fair agreement with the experimental data. However, the whole pattern of predictions has to be understood in detail, especially the interplay between finite volume and conservation laws and the variation of energy density and other parameters with energy. The observed deviations are to be investigated in more detail to check whether they can be attributed to the used approximation. Particularly, we have to assess the effect of using the larger flavour symmetry group SU(3) and the inclusion of resonance interference terms.

Another test of the model has been made comparing measured branching ratios of various heavy resonances ( $m_r \gtrsim 1.6$  GeV) assuming the idea of an identification between extended clusters and resonances (originally put forward by Hagedorn [8]). Also in this case results are encouraging and an overall fair agreement with the data has been found. Still, a better understanding of conservation laws and finite volume effects is needed.

Further tests should be made on other kinds of collision and on  $p\bar{p}$  annihilation. Exclusive channels have been abundantly measured in this reaction, but, unfortunately, the initial protonium atomic state is a poorly known mix of angular momentum and isospin states and a comparison with SHM is more problematic with respect to  $e^+e^-$ .

Another fundamental step is the definition of the channel probability assuming the phase space dominance model enforcing the full set of conservation laws. The comparison between phase space dominance and SHM is actually a crucial test to understand whether exclusive channels can really serve to distinguish between them and to highlight effects of the finite spatial extension of clusters.

## References

- [1] F. Becattini, Z. Phys. C 69 (1996) 485;  
 F. Becattini, Proc. of XXXIII Eloisatron Workshop on "Universality Features in Multihadron Production and the leading effect" (1996) 74, hep-ph 9701275; F. Becattini, U. Heinz, Z. Phys. C 76 (1997) 269;  
 F. Becattini, G. Passaleva, Eur. Phys. J. C 23 (2002) 551.

- [2] P. Braun-Munzinger, J. Stachel, J. P. Wessels and N. Xu, Phys. Lett. B 365 (1996) 1;  
J. Cleymans, D. Elliott, H. Satz and R. L. Thews, Z. Phys. C 74 (1997) 319;  
F. Becattini, J. Manninen and M. Gazdzicki, Phys. Rev. C 73 (2006) 044905;  
W. Broniowski, A. Baran and W. Florkowski, Acta Phys. Polon. B 33 (2002) 4235.
- [3] G. Marchesini, B.R. Webber et al., Comp. Phys. Comm. 67 (1992) 465.
- [4] F. Becattini, U. Heinz, Z.Phys C 76, 269 (1997);  
H. Satz, Nucl. Phys. Proc. Suppl. 94, 204 (2001);  
J. Hormuzdiar, S. D. H. Hsu and G. Mahlon, Int. J. Mod. Phys. E 12, 649 (2003);  
R. Stock, Phys. Lett. B 456, 277 (1999);  
Y. Dokshitzer, Acta Phys. Polon. B 36 361 (2005);  
A. Bialas, Phys. Lett. B 466 301 (1999);  
V. Koch, Nucl. Phys. A 715 108 (2003);  
L. McLerran, arXiv:hep-ph/0311028;  
F. Becattini, J. Phys. Conf. Ser. 5 175 (2005).
- [5] D. Kharzeev, Nucl. Phys. A 774 (2006) 315.
- [6] J. Hormuzdiar, S. D. H. Hsu, G. Mahlon Int. J. Mod. Phys. E 12 (2003) 649.
- [7] U. Heinz, Nucl. Phys. A 661 (1999) 140.
- [8] R. Hagedorn, N. Cim. Suppl. 3 (1965) 147.
- [9] F. Becattini, J. Phys. Conf. Ser. 5 175 (2005).
- [10] W. Blumel, P. Koch, U. Heinz Z. Phys. C 63 (1994) 637.
- [11] F. Becattini, L. Ferroni, Eur. Phys. J. C 35 (2004) 243.
- [12] F. Becattini, L. Ferroni, Eur. Phys. J. C 38 225 (2004).
- [13] F. Becattini, Nucl. Phys. A 702 (2002) 336.
- [14] D. Kharzeev, Eur. Phys. J. A 29 (2006) 83;  
H. Satz, *Invited talk given at the international conference: "Critical Point and Onset of Deconfinement", Florence, Italy, Jul 3-6, 2006.*
- [15] G. Eilam, C. Hojvat, B. Margolis, W. J. Meggs, S. C. Frautschi and M. Pripstein, Lett. Nuovo Cim. 14 (1975) 108;  
W. Ochs, MPI-PAE/Exp El-107 *Invited talk given at Europhysics Study Conf. on Jet Structure from Quark and Lepton Interactions, Erice, Italy, Sep 12-17, 1982;*  
C. E. Carlson and F. Gross, Phys. Rev. D 14 (1976) 1858.
- [16] F. Cerulus, N. Cim. X22, 958-995 (1961).
- [17] K. Werner, J. Aichelin Phys. Rev. C 52 (1995) 1584.
- [18] K. Werner, J. Aichelin, Phys. Rev. C 68 (2003) 024905.
- [19] L. Ferroni *The microcanonical ensemble of the relativistic hadron gas* PhD thesis, University of Florence (2006);  
F. Becattini, L. Ferroni, in preparation.
- [20] L. Landau and E. Lifshitz, *Quantum Electrodynamics*.
- [21] P. Moussa, R. Stora, *Angular Analysis of Elementary Particle Reactions*, in Proceedings of the 1966 International School on Elementary Particles, Hercegovi (Gordon and Breach, New York, London, 1968).

- [22] S. Weinberg, *The Quantum Theory Of Fields* Vol. 1 Cambridge University Press.
- [23] T. Gabbriellini *Studio di un generatore di eventi per il modello statistico di adronizzazione* Diploma thesis (in Italian) University of Florence (2004).
- [24] R. H. C. Cheng, *Communications of the ACM* 21, 317 (1978).
- [25] R. Dashen, S. Ma, H. Bernstein, *Phys. Rev.* 187 345 (1969);  
R. Dashen, R. Rajamaran, *Phys. Rev. D* 10 694 (1974).
- [26] S. Eidelman *et al.* [Particle Data Group], *Phys. Lett. B* 592 (2004) 1.
- [27] D. Bisello *et al.* [DM2 Collaboration], *Phys. Lett. B* 220 (1989) 321.
- [28] J. E. Augustin *et al.*, LAL-83-21 *Contributed to Int. Europhysics Conf. on High Energy Physics, Brighton, England, Jul 20-27, 1983.*
- [29] A. Antonelli *et al.* [DM2 Collaboration], *Z. Phys. C* 56 (1992) 15.
- [30] B. Aubert *et al.* [BABAR Collaboration], *Phys. Rev. D* 70 (2004) 072004.
- [31] C. Bacci *et al.*, *Nucl. Phys. B* 184 (1981) 31.
- [32] A. Cordier, D. Bisello, J. C. Bizot, J. Buon, B. Delcourt, L. Fayard and F. Mane, *Phys. Lett. B* 109 (1982) 129.
- [33] C. Bacci *et al.*, *Phys. Lett. B* 95 (1980) 139.
- [34] B. Aubert *et al.* [BABAR Collaboration], *Phys. Rev. D* 71 (2005) 052001.
- [35] A. Antonelli *et al.*, *Nucl. Phys. B* 517 (1998) 3.
- [36] M. Castellano *et al.* [ADONE collaboration], *Nouvo Cim.* 14A (1973) 1.
- [37] B. Delcourt *et al.*, *Phys. Lett. B* 86 (1979) 395.
- [38] D. Bisello *et al.*, *Nucl. Phys. B* 224 (1983) 379.
- [39] A. Antonelli *et al.*, *Phys. Lett. B* 313 (1993) 283.
- [40] B. Aubert *et al.* [BABAR Collaboration], *Phys. Rev. D* 73 (2006) 052003.
- [41] A. Cordier, D. Bisello, J. C. Bizot, J. Buon, B. Delcourt, L. Fayard and F. Mane, *Phys. Lett. B* 110 (1982) 335.
- [42] A. Antonelli *et al.* [DM2 Collaboration], *Phys. Lett. B* 212 (1988) 133.
- [43] B. Jean-Marie *et al.*, Report No. SLAC-PUB-1711, 1976 (unpublished).
- [44] [BES Collaboration], *Phys. Lett. B* 630 (2005) 14.
- [45] A. Antonelli *et al.*, *Phys. Lett. B* 334 (1994) 431.
- [46] W. M. Yao *et al.* [Particle Data Group], *J. Phys. G* 33 (2006) 1.